SDMS Doc ID 548559

Underwater Acoustic Modeling of Construction Activities

Marine Commerce South Terminal in New Bedford, MA

Submitted to:
Apex Companies, LCC
125 Broad Street, 5th Floor
Boston, MA 02210

Authors:
Marie-Noël R. Matthews
Mikhail Zykov

13 September 2013

P001192
Document 00420
Version 6.0

JASCO Applied Sciences (Canada) Ltd
2305–4464 Markham Street
Victoria, BC V8Z 7X8 Canada
Tel: +1-250-483-3300
Fax: +1-250-483-3301

Document Version Control

Version	Date	Name	Change
0.1	2012 Oct 03	M-N R Matthews	Initial draft–no results. Released to client for review.
1.0	2012 Oct 26	M-N R Matthews	Draft released to client for review.
2.0	2012 Oct 29	M-N R Matthews	Addressed comments from client. Sent to client.
3.0	2012 Nov 15	M-N R Matthews	Addressed comments from client. Sent to client as final version.
4.0	2013 Sep 03	M-N R Matthews	Significant changes in blast estimation approach from previous version (the sections with major changes were highlighted in yellow). Sent to client.
5.0	2013 Sep 9	M-N R Matthews	Revisions applied to Sections 2.2.3, 4.1.3, and 4.2.3, based on EPA comments. Sent to client.
6.0	2013 Sep 13	M-N R Matthews D. Hannay K. Williams	Revisions applied to Sections 2.2.3, 4.1.3, and 4.2.3, based on EPA comments.

Suggested citation:

Matthews, M.-N.R. and M. Zykov. 2013. *Underwater Acoustic Modeling of Construction Activities: Marine Commerce South Terminal in New Bedford, MA*. JASCO Document 00420, Version 6.0. Technical report by JASCO Applied Sciences for Apex Companies, LCC.

Contents

1. INTRODUCTION 1
1.1. Fundamentals of Underwater Acoustics 2
1.1.1. Properties of Sound 3
1.1.2. Acoustic Metrics 4
1.1.2.1. Metrics for Continuous Sound 4
1.1.2.2. Metrics for Impulsive Sound 5
1.1.2.3. Metrics for Explosive Sound 7
1.1.3. Source Level and Transmission Loss 7
1.1.4. Spectral Density and 1/3-Octave Band Analysis 7
1.2. Acoustic Impact Criteria 9
2. METHODS 10
2.1. Model Scenarios 10
2.2. Acoustic Source Levels 10
2.2.1. Pile Driving 10
2.2.2. Rock Removal–Non-Explosive 11
2.2.3. Rock Removal–Explosive 11
2.2.3.1. UnderWater Calculator spreadsheet 12
2.2.3.2. ConWep 13
2.2.3.3. Adjusted efficiency coefficients 14
2.3. Sound Propagation Models 15
2.3.1. Marine Operations Noise Model 15
2.3.2. Cumulative Sound Exposure Levels 16
3. MODEL PARAMETERS 18
3.1. Environmental Parameters 18
3.1.1. Bathymetry 18
3.1.2. Geoacoustics 18
3.1.3. Sound Speed Profile 19
3.2. Geometry and Modeled Volume 20
4. RESULTS 21
4.1. Source Levels 21
4.1.1. Pile Driving 21
4.1.2. Rock Removal–Non-Explosive 22
4.1.3. Rock Removal–Explosive 24
4.2. Sound Fields 25
4.2.1. Pile Driving 26
4.2.2. Rock Removal–Non-Explosive 29
4.2.3. Rock Removal–Explosive 34
LITERATURE CITED 41

Figures

Figure 1. Location of the proposed Marine Commerce Terminal ( ) and the model scenario locations (★) in New Bedford Harbor, MA. 2
Figure 2. Snapshot of the pressure disturbance due to a plane harmonic sound wave. 3
Figure 3. Example waveform showing a continuous noise measurement and the corresponding root-mean-square (rms) sound pressure. 5
Figure 4. Example waveform showing an impulsive noise measurement. Horizontal lines indicate the peak pressure and 90% root-mean-square (rms) pressure for this impulse. The gray area indicates the 90% energy time interval (T_{90}) over which the rms pressure is computed. 6
Figure 5. Example power spectrum of ambient noise and the corresponding 1/3-octave band sound pressure levels. Frequency is plotted on a logarithmic scale, so the 1/3-octave bands are larger at higher frequencies. 8
Figure 6. Diagram of pressure wave paths to a receiver in the water column (not to scale). 14
Figure 7. Peak and root-mean-square (rms) sound pressure level (SPL) and sound exposure level (SEL) versus range from a 20 in^3 airgun array. Solid line is the least squares best fit to rms SPL. Dashed line is the best-fit line increased by 3.0 dB to exceed 90% of all rms SPL values (90th percentile fit) (Ireland et al. 2009, Fig. 10). 16
Figure 8. Sound speed profiles sampled at various locations and times of year within New Bedford Harbor, MA. 20
Figure 9. Estimated 1/3-octave band source level spectra for pile driving operations. 21
Figure 10. Estimated 1/3-octave band source level spectra for cutter-head dredges, clamshell bucket dredges, and a 24-inch hammer drill. 24
Figure 11. Sample modeled pressure waveform at the seabed, at a distance of 38, 80, and 160 ft from the detonation of a 150 lb charge. 25
Figure 12. Pile driving with a vibratory hammer at Site 2: Received maximum-over-depth root-mean-square (rms) sound pressure levels (SPLs). Blue contours indicate water depth in feet. 27
Figure 13. Pile driving with a vibratory hammer at Site 2: Received maximum-over-depth sound level thresholds. Blue contours indicate water depth in feet. 28
Figure 14. Non-explosive rock removal at Site 1: Received maximum-over-depth root-mean-square (rms) sound pressure levels (SPLs). Blue contours indicate water depth in feet. 30
Figure 15. Non-explosive rock removal at Site 1: Received maximum-over-depth sound level thresholds. Blue contours indicate water depth in feet. 31
Figure 16. Non-explosive rock removal at Site 2: Received maximum-over-depth root-mean-square (rms) sound pressure levels (SPLs). Blue contours indicate water depth in feet. 32
Figure 17. Non-explosive rock removal at Site 2: Received maximum-over-depth sound level thresholds. Blue contours indicate water depth in feet. 33
Figure 18. Screenshot of UnderWater Calculator spreadsheet while calculating the adjusted distance (slant range) to the injury criteria of 18.4 psi·ms. 34
Figure 19. Screenshot of UnderWater Calculator spreadsheet while calculating the adjusted distance (slant range) to the injury criteria of 75.6 psi. 35
Figure 20. Small scale contour map for explosive charge at Site 2: Peak pressure threshold of 75.6 psi for explosive charges between 30 and 150 lb. Blue contours indicate water depth in feet. 37
Figure 21. Small scale contour map for explosive charge at Site 2: Impulse level threshold of 18.4 psi·ms for explosive charges between 30 and 150 lb. Blue contours indicate water depth in feet. 38

Figure 22. Large scale contour map for explosive charge at Site 2: Peak pressure threshold of 75.6 psi for explosive charges between 30 and 150 lb. Blue contours indicate water depth in feet..... 39
Figure 23. Large scale contour map for explosive charge at Site 2: Impulse level threshold of 18.4 psi·ms for explosive charges between 30 and 150 lb. Blue contours indicate water depth in feet..... 40

Tables

Table 1. The nominal center frequencies of 1/3-octave bands, from 10 Hz to 20 kHz..... 9
Table 2. List of model scenarios. Site 2 is located at the north edge of proposed South Terminal. Site 1 is located within the northern section of the South Terminal dredge footprint (Figure 1). 10
Table 3. Estimated geoacoustic profile for Sites 1 and 2. Within each sediment layer, parameters vary linearly within the stated range..... 19
Table 4. Estimated geoacoustic parameter for grey granite bedrock (gneiss) found in dredge areas 2 and 3 (Figure 1). 19
Table 5. Dredges specifications. 23
Table 6. Distances to peak pressure injury criterion of 75.6 psi. 36
Table 7. Distances to impulse injury criterion of 18.4 psi•ms. 36

1. Introduction

Construction of the proposed Marine Commerce Terminal (South Terminal) in New Bedford, MA, will require pile driving, non-explosive rock removal, and explosive rock removal. This report presents the results of an underwater acoustic modeling study at the proposed construction site. JASCO Applied Sciences (JASCO) carried out this study for Apex Companies, LCC (Apex) in support of the construction project's biological assessment for the Atlantic sturgeon (*Acipenser oxyrinchus*). Interpretation of potential effects of noise on marine life, including Atlantic sturgeon, is outside the scope of this report.

The model scenarios were chosen to evaluate precautionary distances to threshold levels for each construction activity, at the time of year when the water conditions allow sound to propagate the farthest from the source. Four scenarios were modeled:

- One pile driving scenario at Site 2, along the extended South Terminal bulkhead,
- Two non-explosive rock removal scenarios at Sites 1 and 2, within South Terminal dredge footprint, and
- One explosive rock removal scenario at Site 2 (Figure 1).

The sound levels estimated from this study are presented in two formats: as contour maps of the sound fields that show the directivity and range to various sound level thresholds and as maximum and 95% distances to some sound level thresholds. The distances from the sound sources to sound level thresholds, representing pile driving and non-explosive rock removal operations, are provided for:

- Peak sound pressure level (SPL) of 206 dB re 1 μPa,
- Cumulative sound exposure level (cSEL) of 187 dB re 1 $\mu Pa^2 \cdot s$,
- root-mean-square (rms) SPL from 200 to 120 dB re 1 μPa in 10 dB steps, and
- Sound exposure level (SEL) from 200 to 120 dB re 1 μPa in 10 dB steps (for impulse sound sources only).

The distances to sound level thresholds for the use of explosives are provided for:

- Peak pressure of 75.6 psi, and
- Impulse level of 18.4 psi·ms.

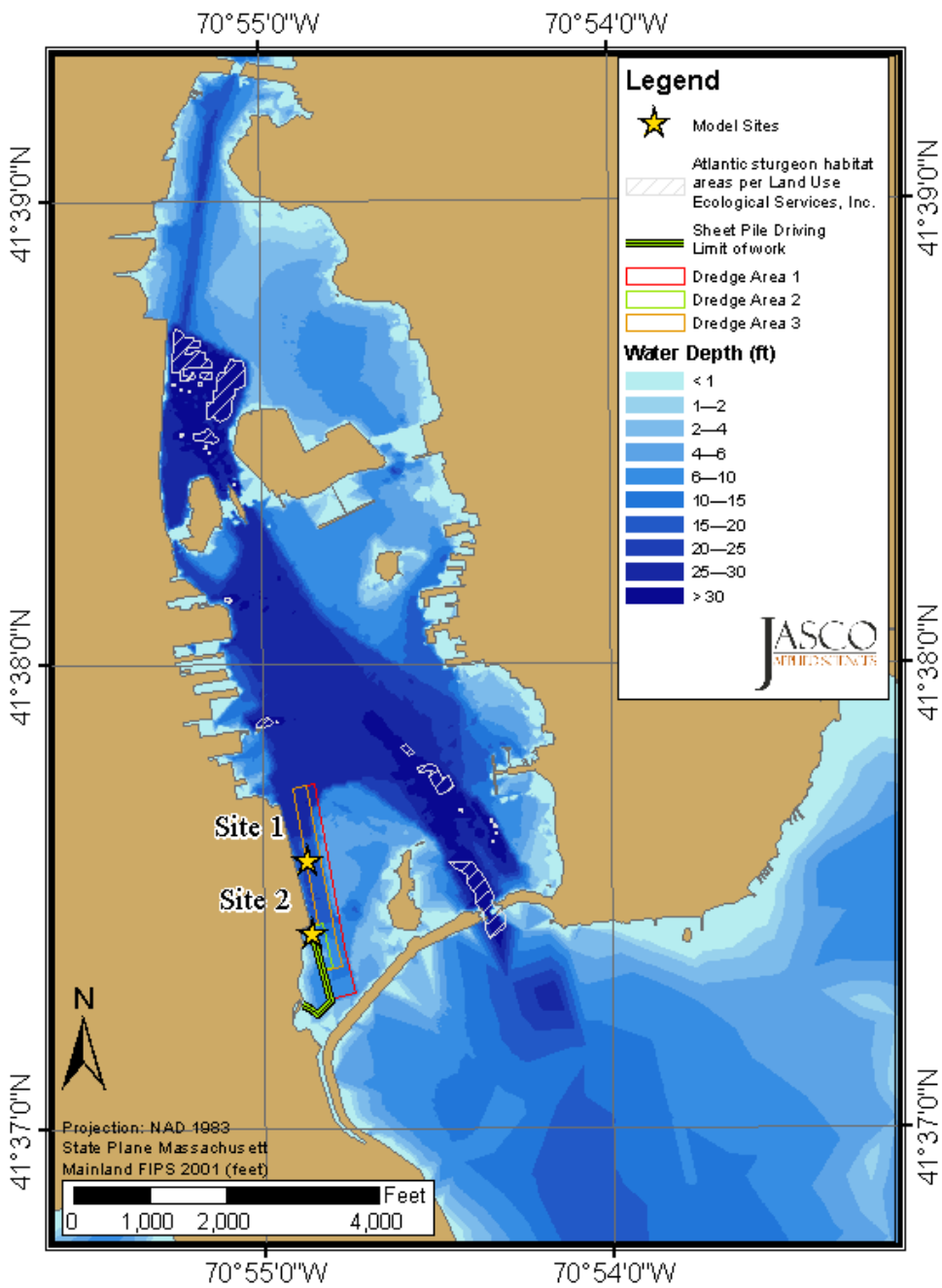

Figure 1. Location of the proposed Marine Commerce Terminal ( ) and the model scenario locations ( ) in New Bedford Harbor, MA.

1.1. Fundamentals of Underwater Acoustics

Sound is the result of mechanical vibration waves traveling through a fluid medium such as air or water. These vibration waves generate a time-varying pressure disturbance that oscillates above and below the ambient pressure. Sound waves may be perceived by the auditory system of an animal, or they may be measured with an acoustic sensor (a microphone or hydrophone). Water conducts sound over four times faster than air due to its lower compressibility; the speed of sound travelling in water is roughly 4900 ft/s, compared to 1100 ft/s in air. Sound is used

extensively by marine organisms for communication and for sensing their environment. Humans may use sound purposely to probe the marine environment through technologies like sonar; more often, human activities such as marine construction produce underwater sound as an unintended side effect.

Sources of underwater sound can be mechanical (e.g., a ship), biological (e.g., a whale) or environmental (e.g., rain). *Noise*, in general parlance, refers to unwanted sound that may affect humans or animals. Noise at relatively low levels can form a background that interferes with the detection of other sounds; at higher levels, noise can also be disruptive or harmful. Common sources of naturally occurring underwater environmental noise include wind, rain, waves, seismic disturbances, and vocalizations of marine fauna. Anthropogenic (i.e., manmade) sources of underwater noise include marine transportation, construction, geophysical surveys, and sonar. Underwater noise usually varies with time and location.

1.1.1. Properties of Sound

The fundamental properties of sound waves are amplitude, frequency, wavelength, and intensity. Frequency of a sound wave, f, is the rate of pressure oscillation per unit of time. Amplitude of a sound wave, A, is the maximum absolute pressure deviation of the wave. If c is the speed of sound in a medium, then the pressure disturbance, P, due to a plane harmonic sound wave (Figure 2) at time t and location x is:

$$P(x,t) = A\cos(2\pi f(x/c - t)) \tag{1}$$

The wavelength, λ, is the distance traveled by a sound wave over one complete cycle of oscillation. For plane harmonic sound waves, the wavelength is equal to the frequency divided by the speed of sound:

$$\lambda = \frac{f}{c} \tag{2}$$

Harmonic waves are fundamentally in acoustics because a well-known mathematical law (Fourier's theorem) states that any arbitrary waveform can be represented by the superposition of harmonic waves.

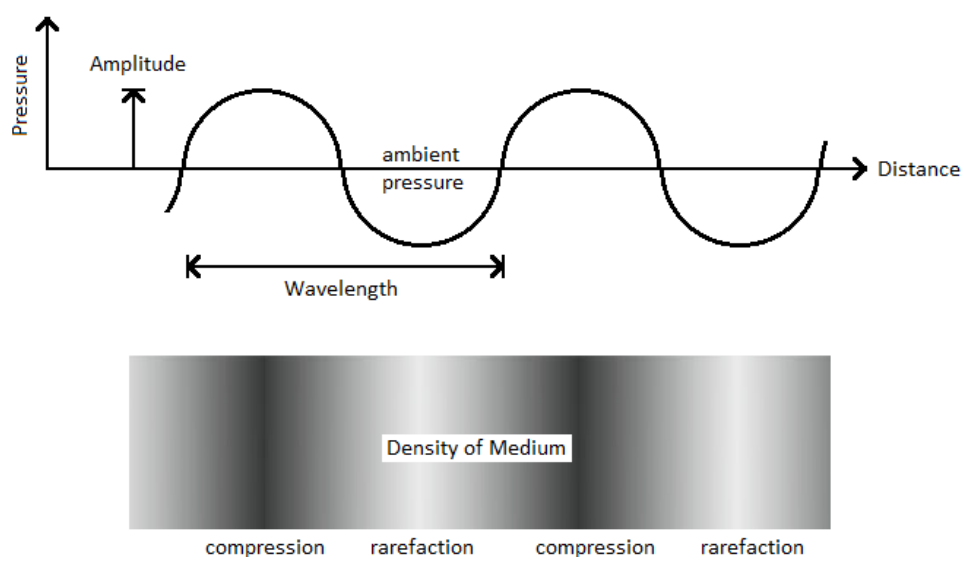

Figure 2. Snapshot of the pressure disturbance due to a plane harmonic sound wave.

The intensity of a traveling sound wave is the acoustic power per unit area carried by the wave. In general, the intensity of a sound wave is related to the wave's amplitude, but it also depends on the compressibility and density of the acoustic medium. The loudness of a sound is related to the intensity; however, loudness is a subjective term that refers to the *perception* of sound intensity, rather than to the actual intensity itself. For humans and other animals, perceived loudness also depends on the frequency and duration of the sound.

1.1.2. Acoustic Metrics

Sound pressure and intensity are commonly measured on the decibel (dB) scale. The decibel scale is a logarithmic scale that expresses a quantity relative to a predefined reference quantity. Sound pressure in decibels is expressed in terms of the sound pressure level (SPL, symbol L_p):

$$L_p = 20\log_{10}\left(P / P_{ref}\right) \tag{3}$$

where P is the pressure amplitude and P_{ref} is the reference sound pressure. For underwater sound, the reference pressure is 1 μPa (i.e., 10^{-6} Pa or 10^{-11} bar). In most cases, sound intensity is directly proportional to the mean square of the sound pressure (i.e., $I \propto \langle P^2 \rangle$); therefore, SPL is considered synonymous with sound intensity level.

The decibel scale for measuring underwater sound is different than for measuring airborne sound. Airborne decibels are based on a standard reference pressure of 20 μPa, which is 20 times greater than the hydroacoustic reference pressure of 1 μPa. Furthermore, due to differences in compressibility and density between the two media, the impedance relationship between sound pressure and sound intensity is different in air than in water. Accounting for these differences in reference pressure and acoustic impedance, for a sound wave with the same intensity in both media, the hydroacoustic decibel value (in dB re 1 μPa) is about 63 dB greater than the airborne decibel value (in dB re 20 μPa).

Sounds that are composed of single frequencies are called "tones." Most sounds are generally composed of a broad range of frequencies ("broadband" sound) rather than pure tones. Sounds with very short durations (less than a few seconds) are referred to as "impulsive." Such sounds typically have a rapid onset and decay. Steady sounds that vary in intensity only slowly with time, or that do not vary at all, are referred to as "continuous."

1.1.2.1. Metrics for Continuous Sound

Continuous sound is characterized by gradual intensity variations over time, e.g., the propeller noise from a transiting ship. The intensity of continuous noise is generally given in terms of the root-mean-square (rms) SPL. Given a measurement of the time varying sound pressure, $p(t)$, for a given noise source, the rms SPL (symbol L_p) is computed according to the following formula:

$$L_p = 10\log_{10}\frac{1}{T}\int_T p(t)^2\,dt / P_{ref}{}^2 \tag{4}$$

In this formula, T is time over which the measurement was obtained. Figure 3 shows an example of a continuous sound pressure waveform and the corresponding rms sound pressure.

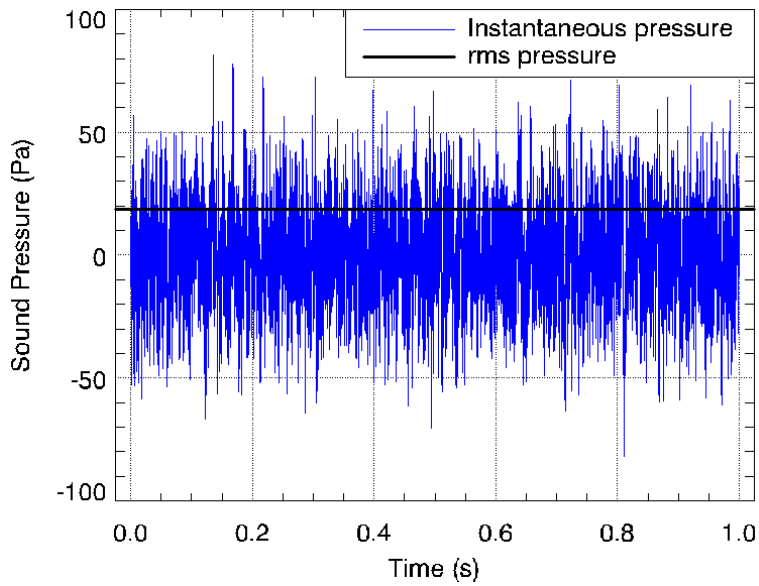

Figure 3. Example waveform showing a continuous noise measurement and the corresponding root-mean-square (rms) sound pressure.

1.1.2.2. Metrics for Impulsive Sound

Impulsive, or transient, sound is characterized by brief, intermittent acoustic events with rapid onset and decay back to pre-existing levels (within a few seconds), e.g., noise from impact pile driving. Impulse sound levels are commonly characterized using three different acoustic metrics: peak pressure, rms pressure, and sound exposure. The peak SPL (symbol L_{pk}) is the maximum instantaneous sound pressure level measured over the impulse duration:

$$L_{\mathrm{pk}} = 20\log_{10}\left(\max\left|p(t)\right| / P_{ref}\right) \tag{5}$$

In this formula, $p(t)$ is the instantaneous sound pressure as a function of time, measured over the impulse duration $0 \le t \le T$. This metric is very commonly quoted for impulsive sounds but does not take into account the duration or bandwidth of the noise.

The rms SPL may be measured over the impulse duration according to the following equation:

$$L_p = 10\log_{10}\left(\frac{1}{T}\int_T p(t)^2\,dt / P_{ref}^2\right) \tag{6}$$

Some ambiguity remains in how the duration T is defined, because in practice the beginning and end of an impulse can be difficult to identify precisely. In studies of impulsive noise, T is often taken to be the interval over which the cumulative energy curve rises from 5% to 95% of the total energy. This interval contains 90% of the total energy (T_{90}), and the SPL computed over this interval is commonly referred to as the 90% rms SPL (L_{p90}). The relative energy, $E(t)$, of the impulse is computed from the time integral of the square pressure:

$$E(t) = \int_0^t p(\tau)^2\,d\tau / P_{ref}^2 \tag{7}$$

According to this definition, if the time corresponding to n% of the total relative energy of the impulse is denoted t_n, then the 90% energy window is defined such that $T_{90} = t_{95}\text{–}t_5$. Figure 4 shows an example of an impulsive sound pressure waveform, with the corresponding peak pressure, rms pressure, and 90% energy time interval.

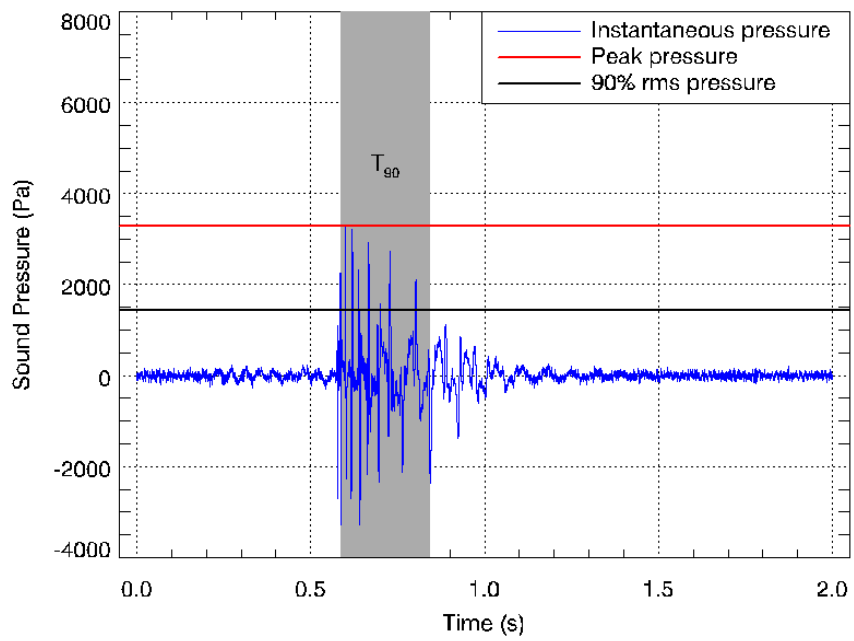

Figure 4. Example waveform showing an impulsive noise measurement. Horizontal lines indicate the peak pressure and 90% root-mean-square (rms) pressure for this impulse. The gray area indicates the 90% energy time interval (T_{90}) over which the rms pressure is computed.

The sound exposure level (SEL, symbol L_E) is a measure of the total sound energy contained in one or more impulses. The SEL for a single impulse is computed from the time-integral of the squared pressure over the impulse duration:

$$L_E = 10\log_{10}\left(\int_{T_{100}} p(t)^2\,dt / P_{ref}^2\right) = 10\log_{10}\left(E\left(T_{100}\right)\right) \tag{8}$$

Unlike SPL, the SEL is generally applied as a dosage metric, meaning that its value increases with the number of exposure events. The cumulative SEL (cSEL) for multiple impulses (symbol $L_E^{(\Sigma)}$) is computed from the linear sum of the SEL values:

$$L_E^{(\Sigma)} = 10\log_{10}\left(\sum_{n=1}^{N} 10^{L_E^{(n)}/10}\right) \tag{9}$$

where N is the total number of impulses, and $L_E^{(n)}$ is the SEL of the nth impulse event. Alternatively, given the mean (or expected) SEL for single impulse events, $\langle L_E \rangle$, the cumulative SEL from N impulses may be computed according the following formula:

$$L_E^{(\Sigma)} = \langle L_E \rangle + 10\log_{10}(N) \tag{10}$$

Sound levels for impulsive noise sources (i.e., impact hammer pile driving) presented in this report refer to single pulse. Because the 90% rms SPL and SEL for a single impulse are both computed from the integral of square pressure, these metrics are related by a simple expression that depends only on the duration of the 90% energy time window T_{90}:

$$L_E = L_{p90} + 10\log_{10}(T_{90}) + 0.458 \tag{11}$$

In this formula, the 0.458 dB factor accounts for the remaining 10% of the impulse energy that is excluded from the 90% time window.

1.1.2.3. Metrics for Explosive Sound

Underwater sound from explosions is most commonly characterized using peak pressure levels (psi), impulse levels (psi·s), or maximum particle velocity (ft/s). In the present report, results are presented in terms of peak pressure and impulse, to conform to the criteria suggested by the National Marine Fisheries Service (Section 1.2).

The peak pressure level is the maximum instantaneous sound pressure level measured over the length of the waveform resulting from an explosion:

$$P_{\mathrm{pk}} = \max\left|p(t)\right| \tag{12}$$

Where $p(t)$ is the instantaneous sound pressure as a function of time.

The impulse is the time integral of pressure through the largest positive phase of a pressure waveform (CSA 2004):

$$I = \int_0^{\tau} p(t)dt \tag{13}$$

In this formula, τ is the end time of the largest positive phase of the pressure waveform. The impulse has units of pounds per square-inch-seconds (psi·s) or pounds per square-inch-milliseconds (psi·ms).

1.1.3. Source Level and Transmission Loss

Sources of underwater noise generate radiating sound waves whose intensity generally decays with distance from the source. The dB reduction in sound level that results from propagation of sound away from an acoustic source is called propagation loss or transmission loss (TL). The loudness or intensity of a noise source is quantified in terms of the source level (SL), which is the sound level referenced to some fixed distance from a noise source. The standard reference distance for underwater sound is 1 m. By convention, transmission loss is quoted in units of dB re 1 m and underwater acoustic source levels are specified in units of dB re 1 μPa at 1 m. In the source-path-receiver model of sound propagation, the received sound level RL at some receiver position **r** is equal to the source level minus the transmission loss along the propagation path between the source and the receiver:

$$\mathrm{RL}(\mathbf{r}) = \mathrm{SL} - \mathrm{TL}(\mathbf{r}) \tag{14}$$

1.1.4. Spectral Density and 1/3-Octave Band Analysis

The discussion of noise measurement presented so far has not addressed the issue of frequency dependence. The sound power per unit frequency of an acoustic signal is described by the power spectral density (PSD) function. The PSD for an acoustic signal is normally computed via the Discrete Fourier Transform (DFT) of time-sampled pressure data. The units of PSD are 1 $\mu\mathrm{Pa}^2$/Hz or dB re 1 $\mu\mathrm{Pa}^2$/Hz. For practical quantitative spectral analysis, a coarser representation of the sound power distribution is often better suited. In 1/3-octave band analysis, an acoustic signal is filtered into multiple, non-overlapping passbands before computing the SPL. These 1/3-octave bands are defined so that three adjacent bands span approximately one octave

(i.e., a doubling) of frequency. Figure 5 shows an example of power spectral density levels and corresponding 1/3-octave band pressure levels for an ambient noise recording.

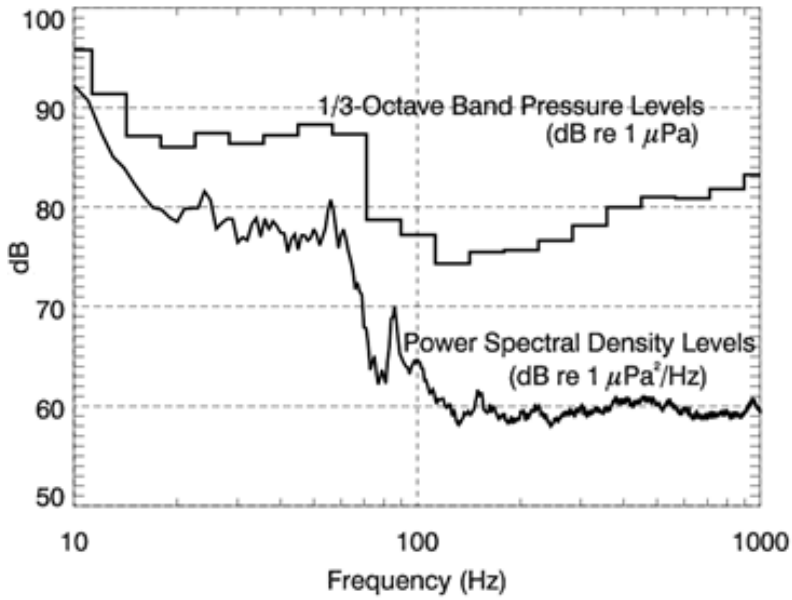

Figure 5. Example power spectrum of ambient noise and the corresponding 1/3-octave band sound pressure levels. Frequency is plotted on a logarithmic scale, so the 1/3-octave bands are larger at higher frequencies.

Standard center frequencies, f_c, for 1/3-octave passbands are given by:

$$f_c(n) = 10^{n/10} \quad n = 1, 2, 3... \tag{15}$$

Nominal 1/3-octave band center frequencies, according to ISO standards, for the range relevant to this study are listed in Table 1. The SPL inside a 1/3-octave band, $L_{pb}(f_c)$, is related to the average PSD level inside that frequency band, $L_{ps}^{(avg)}(f_c)$, by the bandwidth, Δf:

$$L_{ps}^{(avg)}(f_c) = L_{pb}(f_c) - 10\log_{10}(\Delta f) \tag{16}$$

The bandwidth of a 1/3-octave band is equal to 23.1% of the band center frequency (i.e., $\Delta f = 0.231 f_c$). Spectrum density levels and band levels are not limited to measurements of sound pressure: they may also, with appropriate selection of reference units, be given for SEL.

Table 1. The nominal center frequencies of 1/3-octave bands, from 10 Hz to 20 kHz.

Band Number	Center Frequency (Hz)	Band Number	Center Frequency (Hz)	Band Number	Center Frequency (Hz)	Band Number	Center Frequency (Hz)
10	10	20	100	30	1,000	40	10,000
11	12.5	21	125	31	1,250	41	12,500
12	16	22	160	32	1,600	42	16,000
13	20	23	200	33	2,000	43	20,000
14	25	24	250	34	2,500		
15	31.5	25	315	35	3,150		
16	40	26	400	36	4,000		
17	50	27	500	37	5,000		
18	63	28	630	38	6,300		
19	80	29	800	39	8,000		

1.2. Acoustic Impact Criteria

The acoustic impact criteria considered in this report were based on the recommendation from the National Marine Fisheries Service (NMFS). Currently, NMFS has no formal criteria for assessment of injury, mortality, or behavioral effect on fish created by continuous sound; however, NMFS, through correspondence with Apex, requested that the same impact criteria for impact pile driving (i.e., for impulsive sound) be considered for vibratory pile driving and non-explosive rock removal (i.e., for continuous sound). NMFS uses dual criteria for assessment of injury to finfish by impact hammer pile driving. These criteria, derived from the agreement by the Fisheries Hydroacoustic Working Group (FHWG 2008), are:

- Peak SPLs ≥ 206 dB re 1 μPa or cSELs ≥ 187 dB re 1 $\mu Pa^2 \cdot s$ over 24 hours are estimated to create injury or mortality to fish, and
- rms SPLs ≥ 150 dB re 1 μPa are estimated to have behavioral effects on fish.

By convention, SELs for continuous sources are considered over a 1 s interval, thus are equal to rms SPLs (see Section 1.1.2); therefore, distances to the injury or mortality threshold of 187 dB re 1 $\mu Pa^2 \cdot s$ (cSEL over 24 hours) may be greater than that of behavioral effects threshold on fish (rms SPL of ≥ 150 dB re 1 μPa). Although these criteria are unusual for a continuous source[1], these were the only criteria considered in this report.

Currently, NMFS has no formal criteria for assessment of hydroacoustic impacts of underwater explosion on finfish. The peak pressure levels of ≤ 75.6 psi and impulse levels of ≤ 18.4 psi·ms were previously reported to create no injury or mortality to fish (Bullard 2012, Mosher 1999). These levels were therefore used as impact criteria in this report.

[1] The cSEL criteria for nonpulse (continuous) sound are generally much higher than for impulsive sound (by 17 dB for marine mammals; Southall 2007).

2. Methods

2.1. Model Scenarios

Five scenarios were modeled (Figure 1, Table 2):

- one pile-driving scenario,
- two non-explosive rock removal scenarios, and
- one explosive rock removal scenario.

The model scenarios evaluate precautionary distances to sound level thresholds at the time of year when the water conditions allow the sound to propagate the farthest from the source. For comparison purpose, each type of operation was modeled at Site 2 (northern edge of the proposed terminal; Figure 1). Non-explosive rock removal operations were also modeled at Site 1 (within the northern section of the South Terminal dredge footprint; Figure 1).

Table 2. List of model scenarios. Site 2 is located at the north edge of proposed South Terminal. Site 1 is located within the northern section of the South Terminal dredge footprint (Figure 1).

Scenario	Sound Source	Location
Pile Driving		
1	Vibratory hammer	Site 2
Non-Explosive Rock Removal		
2	Cutter-head dredge	Site 1
3	Cutter-head dredge	Site 2
Explosive Rock Removal		
4	Explosive charges (30 to 150 lb)	Site 2

2.2. Acoustic Source Levels

2.2.1. Pile Driving

Documentation provided by Apex specified that sheet piles (type AS-500-12.7 (20 inch) or AZ-14-700 (28 inch)) will be driven to form the bulkhead of the proposed South Terminal. Later, 24–36 inch diameter steel piles will be set into pre-drilled holes in front of the sheet pile. The piles will be driven using a vibratory system; however, the exact drilling equipment was undecided at the time of this study.

The energy required to drive a pile depends on the pile size and the soil resistance encountered; therefore, the noise from the pile driving operations is expected to vary throughout the operation. At first, the pile penetration will be shallow and there will be little soil resistance. At the final stage, when the pile penetration approaches the projected depth, the resistance will be strongest and higher energy is needed to drive the pile. The maximum noise levels from the pile driving are expected at the latest stage of driving for each individual pile (Betke 2008).

Measurements of underwater sound levels reported by Illingworth & Rodkin (2007) were used to estimate sound levels from vibratory hammer on 24-inch sheet piles. Review and analysis of past measurements is currently the best available method for estimating source levels for use in predictive models of pile driving. Technical guidelines generally advocate estimating piling source levels from past measurements (CALTRANS 2009, §4.6.2, WSDOT 2010b, §7.2.4). JASCO has applied this method to several projects to predict the underwater noise from pile driving activities (Gaboury et al. 2007a, 2007b, Austin et al. 2009, Erbe 2009, MacGillivray et al. 2011).

The reported levels were back-propagated to a reference distance of 3.28 ft (1 m) from the source assuming spherical spreading loss ($20\log R$) up to a distance equal to the water depth and cylindrical spreading loss ($10\log R$) thereafter (where R [m] is the range from the source).

2.2.2. Rock Removal–Non-Explosive

A mechanical or hydraulic type dredge with an enclosed bucket will remove surficial sediment within the South Terminal dredge footprint (dredge areas 1–3 in Figure 1). If the rock is too hard for removal with conventional dredges, different non-explosive rock removal techniques may be used, including:

- Hydraulic impact hammering (Hoe Ram),
- Drilling and fracturing of rock,
- Use of large backhoe, and
- Use of a cutter-head.

The exact specification of the non-explosive rock removal equipment was unknown at the time of this study; thus, the estimated source levels from the different activities considered were compared and the “loudest” technique was modeled to present precautionary estimates of radii to level thresholds.

2.2.3. Rock Removal–Explosive

If the desired water depth cannot be reached by non-explosive rock removal methods, explosives may be used to fragment the bedrock and facilitate dredging. The blasting of shallow bedrock is expected to occur in dredge areas 2 and 3 (Figure 1).

The August 2013 Operational Blasting Plan indicates the proposed blast will have the following characteristics:

- A blast will consist of a series of about 40 detonations.
- Charges will consist of Blastex Plus TX (Dyno Nobel Inc.).
- Charge weights per delay will range between 38 and 136 lb.
- Minimum spacing between charges will be 8 ft.
- Minimum delays between detonations will be 25 ms.
- Charges diameters will vary from 3.75 to 5.5 in, with a typical diameter of 4.25 in.

- Boreholes will be drilled to depths of 7–22.8 ft, depending on the area, with a subdrill (depth below the contract elevation) of 6 ft, and a minimum of 24 in of crushed stones to cap the blast hole.
- Charges will be detonated starting offshore and moving inshore.

Previous versions of this report included results for explosive rock removal that included a 12 dB attenuation factor to model a bubble curtain mitigation system. Nützel (2008) demonstrated this attenuation for charges detonated in water or on the seabed. Given that the updated modeling methodology used in the present study results in significantly shorter distances to injury thresholds than previously estimated, the results presented here do not include estimates of the effect of bubble curtain mitigation.

In earlier versions of this modeling study, the specifications of the blast including charge burial parameters were unknown since a blasting plan was not yet available. The peak pressure and impulse of the pressure waveform were predicted with the UnderWater Calculator spreadsheet developed by Dzwilewski and Fenton (2003), which was designed to predict the acoustic impact of pile removal with explosive charges placed inside a pipe pile. We used this approach to produce precautionary estimates of distances to injury criteria by modeling the buried explosive as a charge confined in a 24-inch pile.

As more information about the blasting specifications became available, it was possible to estimate more accurately the pressure wave in the water from a buried explosive with the Conventional Weapons Effects (ConWep) software (Hyde 1988, 1992). The ConWep-modeled pressure waves were used to refine the confinement assumptions for the charge and, thus, adjust parameters in the UnderWater Calculator spreadsheet to provide conservative distances that are more realistic for the specific environment and blast plan.

2.2.3.1. UnderWater Calculator spreadsheet

The Calculator uses empirical equations for the peak pressure (P_{pk}, in psi) and the impulse (I, in psi·ms; Swisdak 1978) from a blast:

$$P_{\mathrm{pk}}(r) = 145.0\, K_P \left(\frac{W^{1/3}}{r} \right)^{\alpha_P} \tag{17}$$

$$I(r) = 145.0\, W^{1/3} K_I \left(\frac{W^{1/3}}{r} \right)^{\alpha_I} \tag{18}$$

where W is the effective weight of the explosive charge (in kilograms), r is the slant range from the blast (in meters), and K_P, K_I, α_P, and α_I are coefficients specific to an explosive.

These equations were developed for a free charge detonated in the water column. The kinetic energy coupled into the water from a charge confined in a pile is reduced because a portion of the blast energy is absorbed by non-elastic deformations of the pile and sediment. To simulate the shock wave from such a detonation, Dzwilewski and Fenton (2003) introduced a multiplier for the charge weight, known as the efficiency coefficient, which yields the effective weight of the confined charge. A charge of the effective weight detonated in water without confinement results in the same peak pressure and impulse as a charge of the total weight confined in a pile.

Dzwilewski and Fenton (2003) performed several numerical model runs with the Eulerian hydrocode CTH, a three-dimensional shock wave physics code (McGlaun et al. 1990), to quantify the explosive coupling efficiency for a charge buried in compact clay sediments and for a charge placed inside a steel pipe driven into clay sediments. For example, for a 50 lb C4 charge in stiff clay sediments the efficiency coefficient was estimated at 79%. When the same charge was placed inside a 36-inch diameter pile with 1.5-inch wall in clay, the efficiency coefficient was reduced to 39% (Dzwilewski and Fenton 2003).

2.2.3.2. ConWep

Depending on the type of substrate material, capping material, charge weight, and burial depth, the effect of a blast in the substrate may be as low as 1.4% compared to the same blast in open water (USACE 1999). Based on the blast specification in the August 2013 Operational Blasting Plan, the efficiency coefficients used in the original study were determined to be too high to accurately estimate the distances to injury criteria. Using ConWep enabled us to estimate more accurately the pressure wave in the substrate and at the seabed. In the current version of the report, the efficiency coefficients in the UnderWater Calculator spreadsheet were adjusted based on ConWep results; this approach provides more realistic, yet still conservative estimates of distances to peak pressure and impulse thresholds.

ConWep uses a set of empirical equations and curves representing the effect from several conventional explosive weapons, including explosives detonated in ground and bedrock, collected by the U.S. Army Corps of Engineers and recorded in the U.S. Army manual TM 5-855-1, *Fundamentals of Protective Design for Conventional Weapons*. ConWep includes a database of the yield and detonation rates for a number of explosive compounds, including ANFO (Ammonium Nitrate/Fuel Oil). In ground shock mode, ConWep predicts the peak pressure and impulse at a chosen target range and depth in the substrate (bedrock). The input parameters include the type of explosive, the charge weight, the geometry of the detonation (depth of the charge, distance to the receiver, and depth of the receiver), and the geoacoustic parameters of the substrate: density, compressional-wave (or P-wave) velocity, and attenuation coefficient.

A pressure wave propagating in the substrate will be partially transmitted to the water through the seabed (Figure 6). The ratio of amplitude of the transmitted wave to the incident wave, denoted as the transfer coefficient (T), was calculated based on the impedance values for the water and substrate layers (Wright and Hopky 1998):

$$\begin{aligned} T &= \frac{2(Z_W / Z_S)}{1+(Z_W / Z_S)} \\ Z_W &= \rho_W c_W / \cos(\theta_W) \\ Z_S &= \rho_S c_S / \cos(\theta_S) \end{aligned} \tag{19}$$

where Z_w and Z_s are the acoustic impedances in the water and substrate, respectively. The acoustic impedance is calculated as a product of density (ρ) and P-wave velocity (c), divided by the cosine of the angle of propagation measured normal to the seabed (θ). To provide conservative estimates of the pressure transferred to the water column, we used the maximum transfer coefficient value at all ranges from the detonation.

According to Snell's law, for incident waves with small grazing angles, i.e., where the pressure wave propagates almost parallel to the seabed ($\theta_S \approx 90°$), the maximum angle of propagation of the transmitted wave is $\theta_W = 30°$. Thus, for small grazing angles, transmitted waves will propagate the farthest in the water. This conservative case was also used for the pressure and impulse calculations.

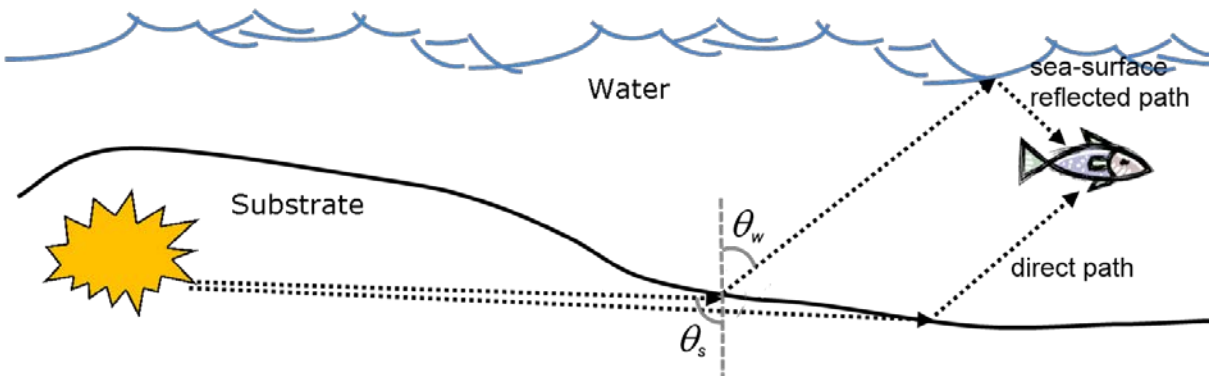

Figure 6. Diagram of pressure wave paths to a receiver in the water column (not to scale).

The transmitted wave, propagating at approximately 60° from the seabed, will be reflected at the water's surface. The sea surface reflections will produce opposite-phase signals that truncate the positive phase of the transmitted direct-path pressure wave, thereby reducing the impulse time integration window (Equation 13), without reducing the peak pressure. By calculating the peak pressure and impulse at the seabed, the time delay between the direct and surface-reflected waves is maximized, thus generating a conservative measure for both peak pressure and impulse.

The approach to shockwave modeling adopted here assumes a flat seabed (constant bathymetry) around the detonation site.

2.2.3.3. Adjusted efficiency coefficients

As detailed above, we used ConWep for each modeled charge weight to calculate the distances at which peak pressure and impulse thresholds are reached. For each charge weight, the efficiency coefficient in the UnderWater Calculator spreadsheet was adjusted to produce distances consistent with the ConWep results but with the addition of a conservative margin (5–10% of the distance). Since the estimated distances to the impulse threshold are larger than for peak pressure, this metric was used as reference to correlate the results from the UnderWater Calculator spreadsheet to those from ConWep. The resulting adjusted efficiency coefficients were then used to calculate the distances to peak pressure with the UnderWater Calculator spreadsheet.

For each charge weight, the final adjusted distances were obtained as follow:

- The weight the charge was input into the UnderWater Calculator spreadsheet.
- The impulse level was fixed to 18.4 psi·ms.
- The efficiency coefficient was reduced until the distance to the impulse level was within 5–10% larger than that estimated by ConWep.
- The efficiency coefficient was then fixed.
- The distance was reduced until the peak pressure level reached 75.6 psi.

A detailed example of this procedure is presented in the results section (Section 34).

2.3. Sound Propagation Models

Underwater sound propagation (i.e., transmission loss) at frequencies of 10 Hz to 20 kHz was predicted with JASCO's Marine Operations Noise Model (MONM). MONM computes received SEL for directional impulsive sources at a specified source depth.

2.3.1. Marine Operations Noise Model

At frequencies ≤ 2 kHz, MONM computes acoustic propagation via a wide-angle parabolic equation solution to the acoustic wave equation (Collins 1993) based on a version of the U.S. Naval Research Laboratory's Range-dependent Acoustic Model (RAM), which has been modified to account for an elastic seabed. The parabolic equation method has been extensively benchmarked and is widely employed in the underwater acoustics community (Collins et al. 1996). MONM-RAM accounts for the additional reflection loss at the seabed due to partial conversion of incident compressional waves to shear waves at the seabed and sub-bottom interfaces, and it includes wave attenuations in all layers. MONM incorporates the following site-specific environmental properties: a bathymetric grid of the modeled area, underwater sound speed as a function of depth, and a geoacoustic profile based on the overall stratified composition of the seafloor.

MONM-RAM's predictions have been validated against experimental data in several sound source verification programs conducted by JASCO (Hannay and Racca 2005, Aerts 2008, Funk et al. 2008, Ireland et al. 2009, O'Neill et al. 2010, Warner et al. 2010).

At frequencies ≥2 kHz, MONM employs the widely-used BELLHOP Gaussian beam ray-trace propagation model (Porter and Liu 1994) and accounts for increased sound attenuation due to volume absorption at these higher frequencies following Fisher and Simmons (1977). This type of attenuation is significant for frequencies higher than 5 kHz and cannot be neglected without noticeable effect on model results at long ranges from the source. MONM-BELLHOP accounts for the source directivity, specified as a function of both azimuthal angle and depression angle. MONM-BELLHOP incorporates site-specific environmental properties such as a bathymetric grid of the modeled area and underwater sound speed as a function of depth. In contrast to MONM-RAM, the geoacoustic input for MONM-BELLHOP consists of only one interface, namely the sea bottom. This is an acceptable limitation because the influence of the bottom sub-layers on the propagation of acoustic waves with frequencies above 2 kHz is negligible.

MONM computes acoustic fields in three dimensions by modeling transmission loss within two-dimensional (2-D) vertical planes aligned along radials covering a 360° swath from the source, an approach commonly referred to as N×2-D. These vertical radial planes are separated by an angular step size of $\Delta\theta$, yielding $N = 360°/\Delta\theta$ number of planes.

MONM treats frequency dependence by computing acoustic transmission loss at the center frequencies of 1/3-octave bands. Sufficiently many 1/3-octave bands, starting at 10 Hz, are modeled to include the majority of acoustic energy emitted by the source. At each center frequency, the transmission loss is modeled within each vertical plane (N×2-D) as a function of depth and range from the source. Third-octave band received (per-pulse) SELs are computed by

subtracting the band transmission loss values from the directional source level (SL) in that frequency band. Composite broadband received SELs are then computed by summing the received 1/3-octave band levels.

The received SEL sound field within each vertical radial plane is sampled at various ranges from the source, generally with a fixed radial step size. At each sampling range along the surface, the sound field is sampled at various depths, with the step size between samples increasing with depth below the surface. The step sizes are chosen to provide increased coverage near the depth of the source and at depths of interest in terms of the sound speed profile. The received SEL at a surface sampling location is taken as the maximum value that occurs over all samples within the water column below, i.e., the maximum-over-depth received SEL. These maximum-over-depth SELs are presented as color contours around the source.

An inherent variability in measured sound levels is caused by temporal variability in the environment and the variability in the signature of repeated acoustic impulses (sample sound source verification results are presented in Figure 7). While MONM's predictions correspond to the averaged received levels, precautionary estimates of the radii to sound level thresholds are obtained by shifting the best fit line (solid line in Figure 7) upward so that the trend line encompasses 90% of all the data (dashed line in Figure 7).

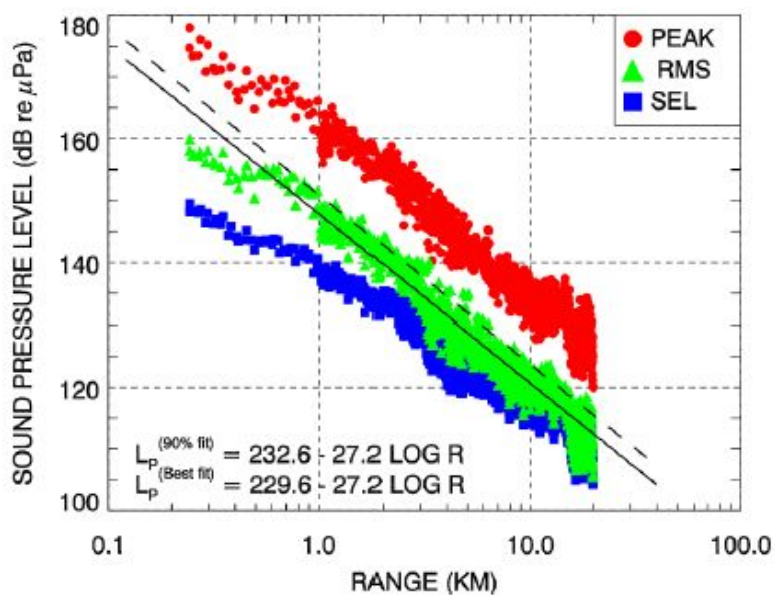

Figure 7. Peak and root-mean-square (rms) sound pressure level (SPL) and sound exposure level (SEL) versus range from a 20 in^3 airgun array. Solid line is the least squares best fit to rms SPL. Dashed line is the best-fit line increased by 3.0 dB to exceed 90% of all rms SPL values (90th percentile fit) (Ireland et al. 2009, Fig. 10).

2.3.2. Cumulative Sound Exposure Levels

While some impact criteria are based on per-pulse received energy at the subject's location, others account for the total acoustic energy to which marine life is subjected over a 24 h period. An accurate assessment of the cumulative acoustic field depends not only on the parameters of each pulse, but also on the number of pulses delivered in a given time period and the relative source position of the pulse. Quite a different issue, which is not considered here but bears

mentioning as a qualifier to any estimates, is that individuals of most species would not remain stationary throughout the accumulation period, so their dose accumulation would depend also on their motion.

For vibratory pile driving and non-explosive rock removal operations that produce continuous not impulsive sound, cSEL is calculated by summing (on a logarithmic scale) the SEL that represents 1 s of operation over the total number of operational seconds expected in 24 hours.

3. Model Parameters

3.1. Environmental Parameters

3.1.1. Bathymetry

Water depths throughout the modeled area were obtained from soundings collected by the U.S. Army Corps of Engineers in support of the New Bedford Harbor Superfund Project. These soundings were adjusted to match proposed dredged depth in the pile driving area. In areas where no soundings were available, data were obtained from STRM30+ (v7.0), a global topography and bathymetry grid with a resolution of 30 arc-seconds or about 2,300 × 6,000 ft (700 × 1,800 m) at the studied latitude (Rodriguez et al. 2005).

Bathymetry for a 10 × 12 miles (16 × 19 km) area, including waters from the Acushet River to Buzzards Bay, was re-gridded by minimum curvature gridding onto a Universal Transverse Mercator (UTM) Zone 19 projection with a horizontal resolution of 6.6 × 6.6 ft (2 × 2 m). Note that all maps presented in this report were projected onto the horizontal datum NAD 1983 U.S. State Plane Massachusetts Mainland Zone 19 (feet).

3.1.2. Geoacoustics

MONM assumes a single geoacoustic profile of the seafloor for the entire model area. The acoustic properties required by MONM are:

- sediment density,
- compressional-wave (or P-wave) sound speed,
- P-wave attenuation in decibels per wavelength,
- shear-wave (or S-wave) speed, and
- S-wave attenuation, in decibels per wavelength.

The geological stratification in New Bedford Harbor was based on boring logs provided by Apex. In general, dark grey sand with some grey to black organic silt was found down to 10–35 ft below the mudline. Based on the available data, this layer was averaged to 21 ft below the mudline for modeling purposes. Throughout the harbor, fractured grey granite bedrock (gneiss) is found directly below the silty sand layer. Seismic refraction data collected by Northeast Geophysical Services in March 2011 provided estimates of P-wave sound speed in this gneiss layer.

The other necessary acoustic properties were estimated from the geological stratification and sound speed data provided by Apex and values from analysis of similar material by Hamilton (1980), Ellis and Hughes (1989), and Barton (2007).

Table 3 presented the geoacoustic profile used by the sound propagation model MONM. Table 4 presents the geoacoustic parameters used by the semi-empirical model ConWep.

Table 3. Estimated geoacoustic profile for Sites 1 and 2. Within each sediment layer, parameters vary linearly within the stated range.

Depth below seafloor (ft)	Material	Density (lb/ft^3)	P-wave speed (ft/s)	P-wave attenuation (dB/λ)	S-wave speed (ft/s)	S-wave attenuation (dB/λ)
0-21	Sand and some black organic silt	110.5-121.7	5,331-7,150	0.96-1.10	1,180	4.8
21-27	Grey granite Gneiss	162.3	10,250-16,807	0.275		
≥ 27	Grey granite Gneiss	162.3	16,807	0.275		

Table 4. Estimated geoacoustic parameter for grey granite bedrock (gneiss) found in dredge areas 2 and 3 (Figure 1).

Material	Density (lb/ft^3)	P-wave speed (ft/s)	Attenuation coefficient
Grey granite gneiss	162.3	10,250	1.9

3.1.3. Sound Speed Profile

The sound speed profiles for the modeled sites were derived from sound speed profile data provided by Apex (Figure 8). These profiles were verified against temperature and salinity profiles from the US Naval Oceanographic Office's *Generalized Digital Environmental Model V 3.0* (GDEM; Teague et al. 1990, Carnes 2009). GDEM provides ocean climatology of temperature and salinity for the world's oceans on a latitude-longitude grid with 0.25° resolution, with a temporal resolution of one month, based on global historical observations from the US Navy's Master Oceanographic Observation Data Set (MOODS). The climatology profiles include 78 fixed depth points, up to a maximum depth of 22,310 ft (6,800 m) (where the ocean is that deep), including 55 standard depths between 0 and 6,562 ft (2,000 m). The GDEM temperature-salinity profiles were converted to sound speed profiles according to the equations of Coppens (1981):

$$\begin{aligned} c(z,T,S,\phi) &= 1449.05 + 45.7t - 5.21t^2 - 0.23t^3 \\ &\quad + \left(1.333 - 0.126t + 0.009t^2\right)\left(S - 35\right) + \Delta \\ \Delta &= 16.3Z + 0.18Z^2 \\ Z &= \frac{z}{1000}\left(1 - 0.0026\cos(2\phi)\right) \\ t &= \frac{T}{10} \end{aligned} \tag{20}$$

where z is water depth (m), T is temperature (°C), S is salinity (psu), and ϕ is latitude (radians).

The same monthly variations were observed in both Apex and GDEM data. Since Apex data were sampled within the New Bedford Harbor, and GDEM data were only available within Buzzard Bay, Apex's sound speed profiles are used to provide a more accurate estimate of the sound speed at the South Terminal Project sites.

To provide precautionary estimates of distances to level thresholds, sound propagation was modeled for the month of September (yellow, Figure 8). The sound speed profile in fall becomes

slightly upward refractive, which promotes sound propagation by reducing interactions with the seabed.

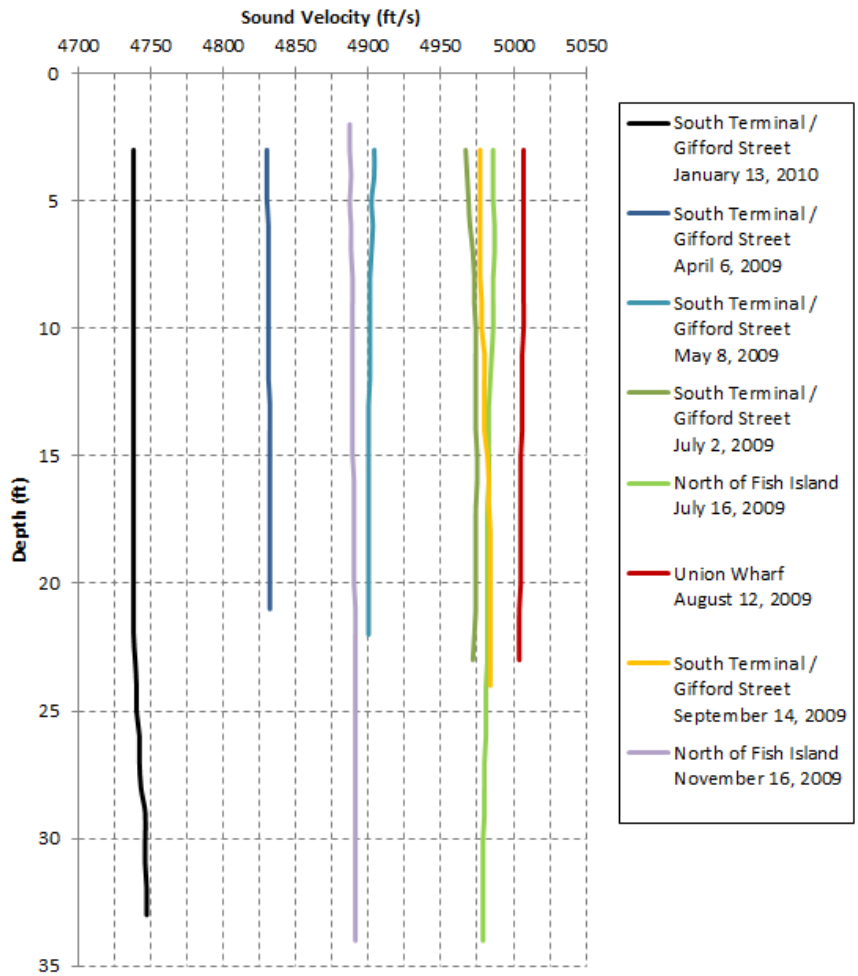

Figure 8. Sound speed profiles sampled at various locations and times of year within New Bedford Harbor, MA.

3.2. Geometry and Modeled Volume

The sound fields were modeled over New Bedford Harbor on an area about 13,123 × 23,950 ft (4.0 × 7.3 km), with a horizontal separation of 6.6 ft (2 m) between receiver points along the modeled radials. Sound fields were modeled with a horizontal angular resolution of $\Delta\theta = 2.5$, for a total of $N = 144$ radial planes. The receiver depths span the entire water column over the modeled areas, from 1 to 164 ft (0.3 to 50 m), with step sizes that increased from 0.3 to 16.4 ft (0.1 to 5 m), with increasing depth.

4. Results

4.1. Source Levels

4.1.1. Pile Driving

Blackwell et al. (2007) provided received sound level spectra from vibratory pile driving. This spectrum revealed distinct peaks in the 1/3–octave bands centered at 16, 31.5, and 50 Hz, which are consistent with the vibration frequency of about 30 Hz. The spectrum was scaled to a broadband level equal to the maximum source level for vibratory pile driving a 24-inch (0.6 m) pile reported by Illingworth & Rodkin (2007): 185 dB re 1 $\mu Pa^2 \cdot s$.

Since the 24–36 inch diameter steel piles are to be set into pre-drilled holes, 1/3-octave bands source levels were also estimated for the drilling operation. JASCO recorded a Beetle (hammer) drill with a drill bit diameter of 24 inches passing through metamorphic rock (Mouy and Zykov 2009). The drill rig was installed on a temporary metal frame resting on the river bottom. This hammer-drilling operation and environment are expected to be representative of the activities proposed for the New Bedford terminal.

Figure 9 presents resultant source level spectra in 1/3-octave bands. Since the broadband levels are estimated higher for pile driving operations than for drilling operations, the spectrum for vibratory hammers was used in this study.

As the pile flexes under the action of the pile driver, its entire length excites pressure waves in the water, meaning that the pile is a distributed sound source. Because of losses from bottom and surface interactions, attenuation will be less for a source at mid-depth than for one near the seafloor or surface. The pile was approximated by a point source located at half the water depth. This positioning of the equivalent point source is estimated to result in precautionary distances to sound level thresholds.

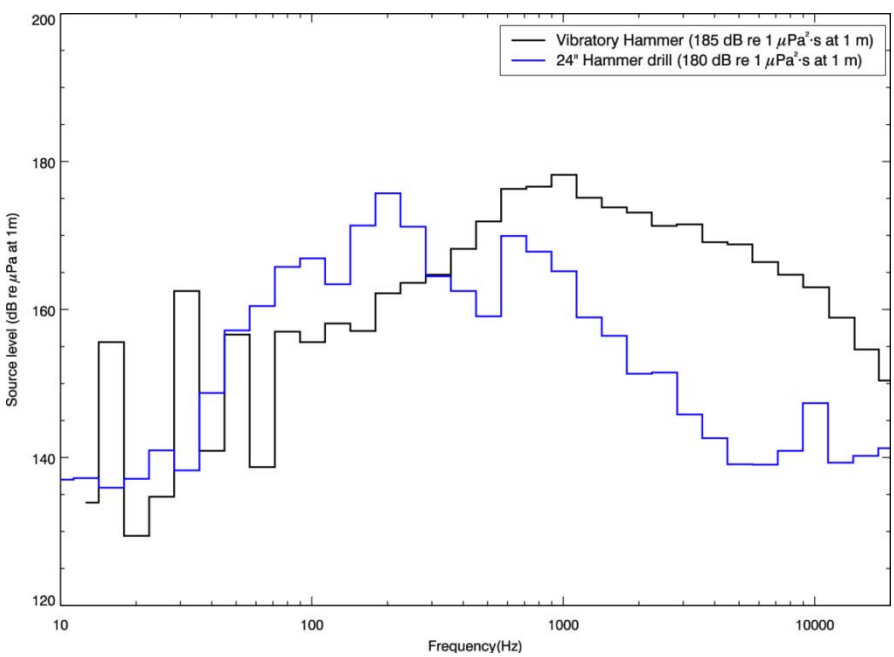

Figure 9. Estimated 1/3-octave band source level spectra for pile driving operations.

4.1.2. Rock Removal–Non-Explosive

Since underwater spectrum representing hydraulic impact hammering (Hoe Ram) and drilling and fracturing of metamorphic rock were not found in the literature, a Beetle (hammer) drill with a drill bit diameter of 24 inches passing through metamorphic rock (Mouy and Zykov 2009), was used as proxy for the two types of activities.

A cutter-head may also be used to help loosen the sediments. The head can usually be steered using cables and winches or thrusters. Generally, cutter-head dredges do not have a propulsion system, but use *legs*, known as spuds, to swing between anchors, or may use service tugs. The major source of noise is generated by the impact and abrasion of the sediment passing through the cutter-head, suction pipe, and pump (Robinson et al. 2011).

Backhoe dredgers are relatively quiet compared to other dredges (CEDA 2011). The noise sources from backhoe dredging are the barge-installed power plant and scraping sounds as the bucket digs into hard sediment. Backhoe and bucket dredgers have a similar setup: a crane installed on a barge. The only difference being that the bucket is controlled through a steel wire cable instead of a rigid arm. Since noise measurements of a backhoe dredger were unavailable, clamshell bucket dredge measurements were used as proxy.

One dredging duty cycle for a clamshell bucket dredge involves the following events:

- Bucket striking the bottom,
- Bucket digging into the bottom/bucket closing,
- Winching up, and
- Dumping the material from the bucket.

Dickerson et al. (2011) identified that the noisiest event is the bucket striking the bottom. This acoustic event is very short compared to the length of a duty cycle (~1 min), and happens once per duty cycle. The source levels for other events are at least 6 dB lower. Table 5 presents the specification for the cutter-head and clamshell bucket dredges considered in this study. Figure 10 presents the 1/3-octave band source level spectra for cutter-head dredges, clamshell bucket dredges, and a 24-inch hammer drill.

Table 5. Dredges specifications.

Dredge Name	Type	Length × breadth × draft (ft)	Capacity	Pump power (kW)	Dredging depth (ft)	Estimated rms SPL broadband level (dB re 1 µPa @ 1 m)	Reference
JFJ de Nul	Cutter-head suction dredge using thruster to move cutter-head	408 × 91 × 21	unknown	Cutter drive: 6000 Submerged dredge pump on cutter ladder: 3800 Inboard dredge pumps: 2 x 6000 Propulsion: 2 x 3800 Total installed power: 27 190	19 (min) 115 (max)	179.6	Hannay et al. 2004 and Sakhalin Energy
Aquarius	Self-propelled Cutter-head suction dredge using thrusters to move cutter-head	351 × 62 × 16	unknown	unknown	82 (max)	185.5	Malme et al. 1989
Columbia	Cutter-head suction dredge using winch to move cutter-head	160 × 44 × 7	unknown	Cutter power: 375 Total power: 3954 Pipe Diameter: 2 ft	59 (max)	181.8	McHugh et al. 2007
Beaver MacKenzie	Cutter-head suction dredge using winch to move cutter-head	284 × 51 × 13	Gross tonnage: 2148.5 t	Ladder: 1119 (1500 hp) Discharge: 1268 (1700 hp) jet pump: 1119 (1500 hp) Pipe Diameter: 2.8 ft	148 (max)	172.1	Malme et al. 1989
Viking	Clamshell bucket dredge	260 × 66 × 6	Maximum lift : 136 t	unknown	unknown	169.5	Dickerson et al. 2001
Argilopotes	Clamshell bucket dredge	unknown	unknown	unknown	unknown	167.6	Miles et al. 1987

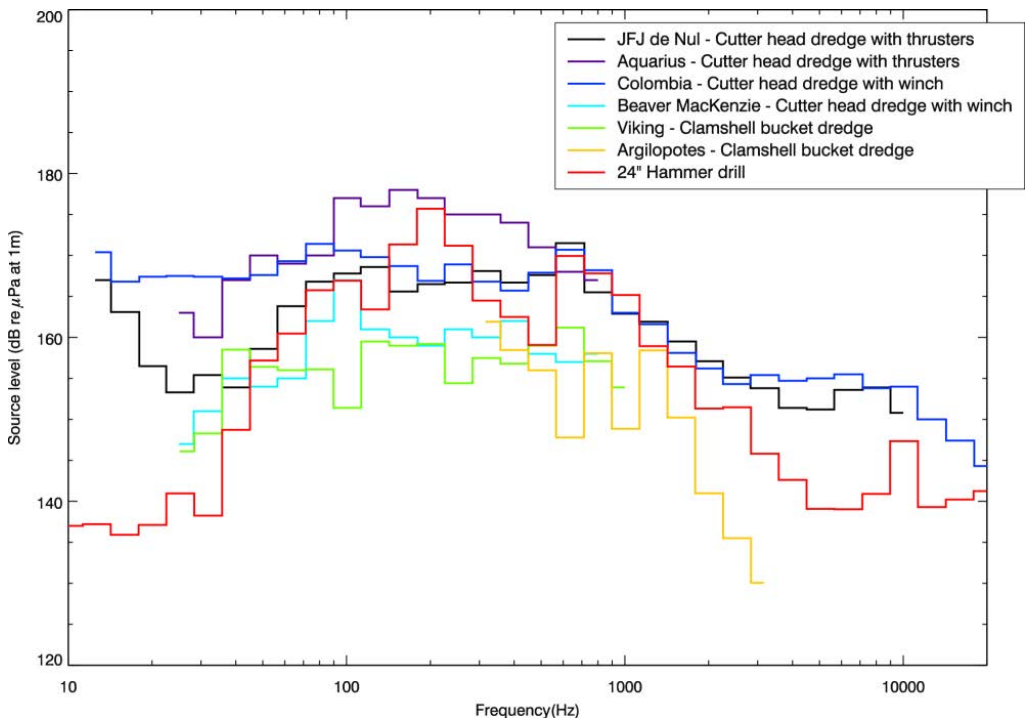

Figure 10. Estimated 1/3-octave band source level spectra for cutter-head dredges, clamshell bucket dredges, and a 24-inch hammer drill.

Sound levels from the cutter-head dredge Aquarius were used in this study, since they represents the highest broadband source levels (185.5 dB re 1 µPa @ 1 m). As the available spectrum for Aquarius does not include frequencies above 800 Hz, source levels at higher frequencies were estimated using the highest values in each 1/3-octave band between the cutter-head dredges JFJ de Nul and Colombia.

Because losses from bottom and surface interactions will be less for a source at mid-depth than for one near the seafloor or surface, the sound of non-explosive rock removal activities was approximated by a point source located at half the water depth. This positioning of the equivalent point source is estimated to produce results in precautionary distances to level thresholds.

4.1.3. Rock Removal–Explosive

In the original study (as described in version 3.0 of this report), the peak pressure and impulse of the pressure wave from explosive rock removal operations were predicted with UnderWater Calculator spreadsheet (Dzwilewski and Fenton 2003). The calculations (Equations 17 and 18) were done for distances extending as far as 4500 ft from the detonation point. Scenarios with charge sizes of 30, 50, 100, 130, and 150 lb were considered, based on the assumption of confinement by a 24-inch diameter pile with a 1-inch thick wall in stiff clay. The efficiency coefficient for such detonations was estimated to range from 38.0% for a 30 lb charge to 52.4% for a 150 lb charge.

The current blast specification (Section 2.2.3) prescribes Blastex Plus TX explosive. Since this material is not in the ConWep database, ANFO was used in the model as the charge material. The material safety data sheet for Blastex Plus TX indicates it is made of a similar material to

ANFO, but specially packed for use in wet environments. Five charge weights (30, 50, 100, 130, and 150 lb) were modeled. Based on the information in the August 2013 Operational Blasting Plan, the top of the charge would be positioned between 3 and 18.8 ft below the seafloor (considering overburden and capping material). On precautionary grounds, the detonation depth was modeled at the shallowest burial depth (3 ft) since a shallower detonation is expected to produce higher peak pressure and impulse levels in the water.

The ConWep-modeled pressure waves for each charge size (see Figure 11 for an example of modeled pressure waves at 38, 80, and 160 ft from a 150 lb charge) were computed at several ranges from the detonation to find the maximum extent of the zone of injury, based on the NMFS criteria. The threshold distances for the impulse metric were then used to calculate adjusted efficiency coefficients for the UnderWater Calculator spreadsheet. These adjusted efficiency coefficients for a charge placed inside bedrock vary between 5.5% for a 30 lb charge and 2.25% for a 150 lb charge. The inverse relation of the adjusted coefficients to charge size is a numerical consequence of the compensation of UnderWater Calculator results to match ConWep. The relatively lower efficiency for larger charges could be due to the inability of the steel pipe of pipe-enclosed charges to effectively constrain larger charge sizes. Even relatively large charges are likely quite well constrained when capped in drilled holes in the seabed and rock.

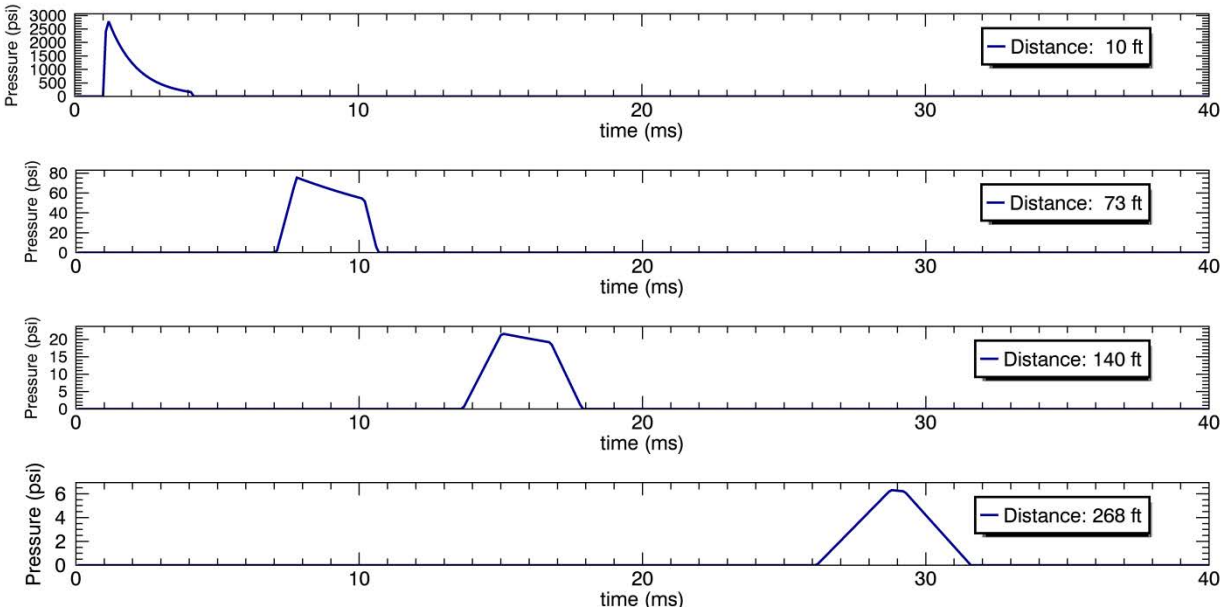

Figure 11. Sample modeled pressure waveform at the seabed, at a distance of 38, 80, and 160 ft from the detonation of a 150 lb charge.

4.2. Sound Fields

It is important to note that several assumptions were made to estimate precautionary distances to sound level thresholds. In addition to the assumptions detailed in Sections 2, 3, and 4.1, the water column was assumed free of obstructions such as construction barges or other vessels that could act as partial noise barriers, depending on their draft. The underwater sound fields predicted by the propagation model were also sampled such that the received sound level at each point in the

horizontal plane was taken to be the maximum value over all modeled depths for that point (see Section 2.3.1).

The predicted distances to specific sound level thresholds were computed from the maximum-over-depth sound fields. The model results are presented as contour maps of maximum-over-depth rms SPL in 10 dB steps, and contours to maximum-over-depth peak SPL, cSEL, and rms SPL thresholds, or peak pressure and impulse level thresholds. Distances to specified threshold are recorded in the legend of the contour maps for pile driving and non-explosive rock removal operations, and tabulated for rock removal operations using explosives.

For pile driving and non-explosive rock removal operations, two distances from the source are reported for sound levels representing the selected impact criteria: (1) R_{max}, the maximum range at which the given sound level was encountered in the modeled sound field; and (2) $R_{95\%}$, the maximum range at which the given sound level was encountered after exclusion of the 5% farthest such points. This definition is meaningful in terms of impact on marine life, because, regardless of the geometric shape of the noise footprint for a given sound level threshold, $R_{95\%}$ is the predicted range encompassing at least 95% of animals of a uniformly distributed population would be exposed to sound at or above that level.

4.2.1. Pile Driving

Apex estimates that each pile will to be driven into place in about 10 min using a vibratory hammer. Cumulative SEL was calculated assuming 10 min of vibratory hammer pile driving operation for each of the 16 piles to be driven in a 24-hour period. Thus, cSELs presented here assume 9600 s of operation in 24 hours. Peak SPL for vibratory pile driving is not expected to reach 206 dB re 1 μPa.

Figure 12 presents a contour map of the modeled rms SPL for pile driving operation with vibratory hammer. Figure 13 presents a contour map of the modeled sound level thresholds for that type operation.

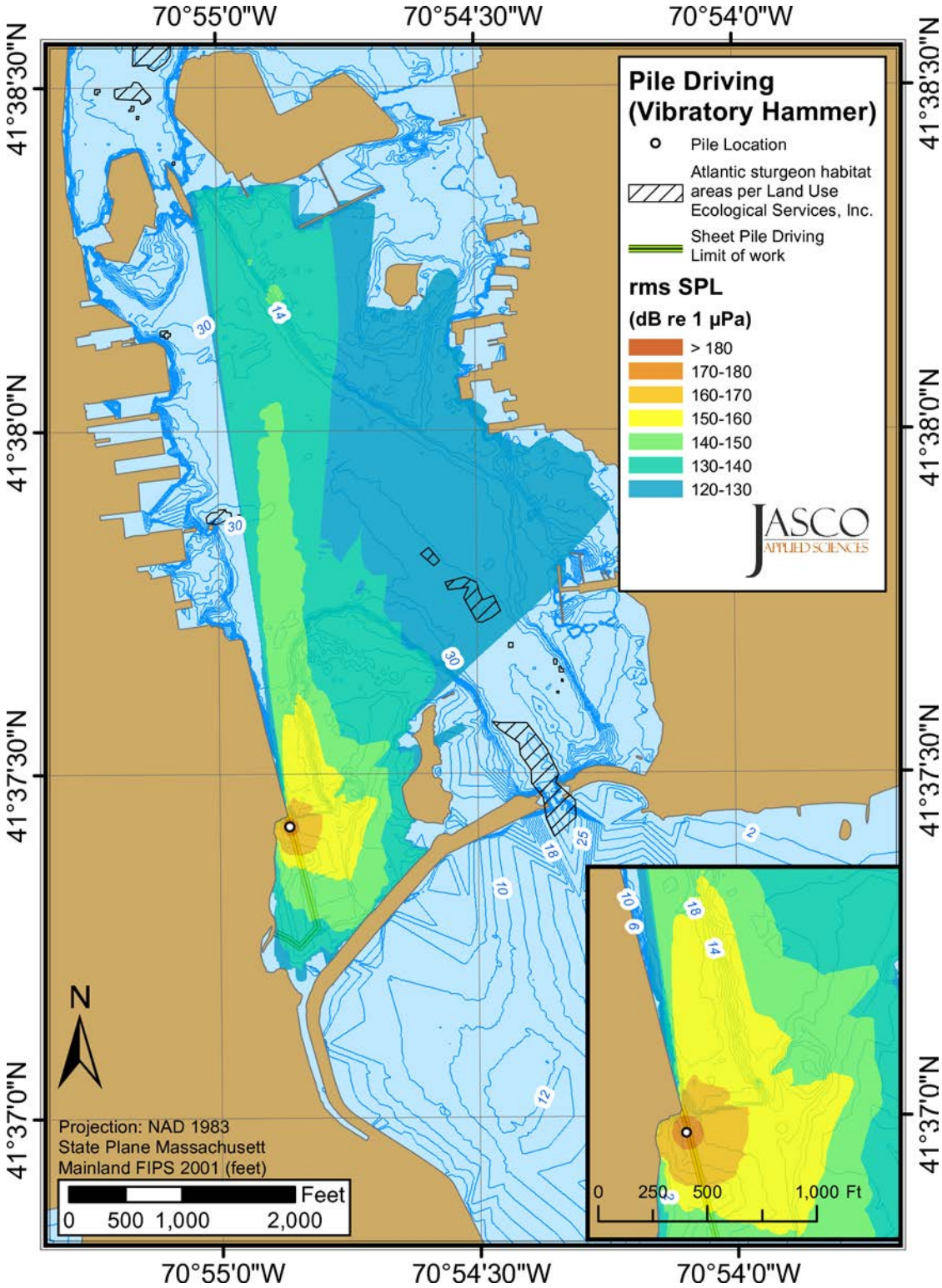

Figure 12. Pile driving with a vibratory hammer at Site 2: Received maximum-over-depth root-mean-square (rms) sound pressure levels (SPLs). Blue contours indicate water depth in feet.

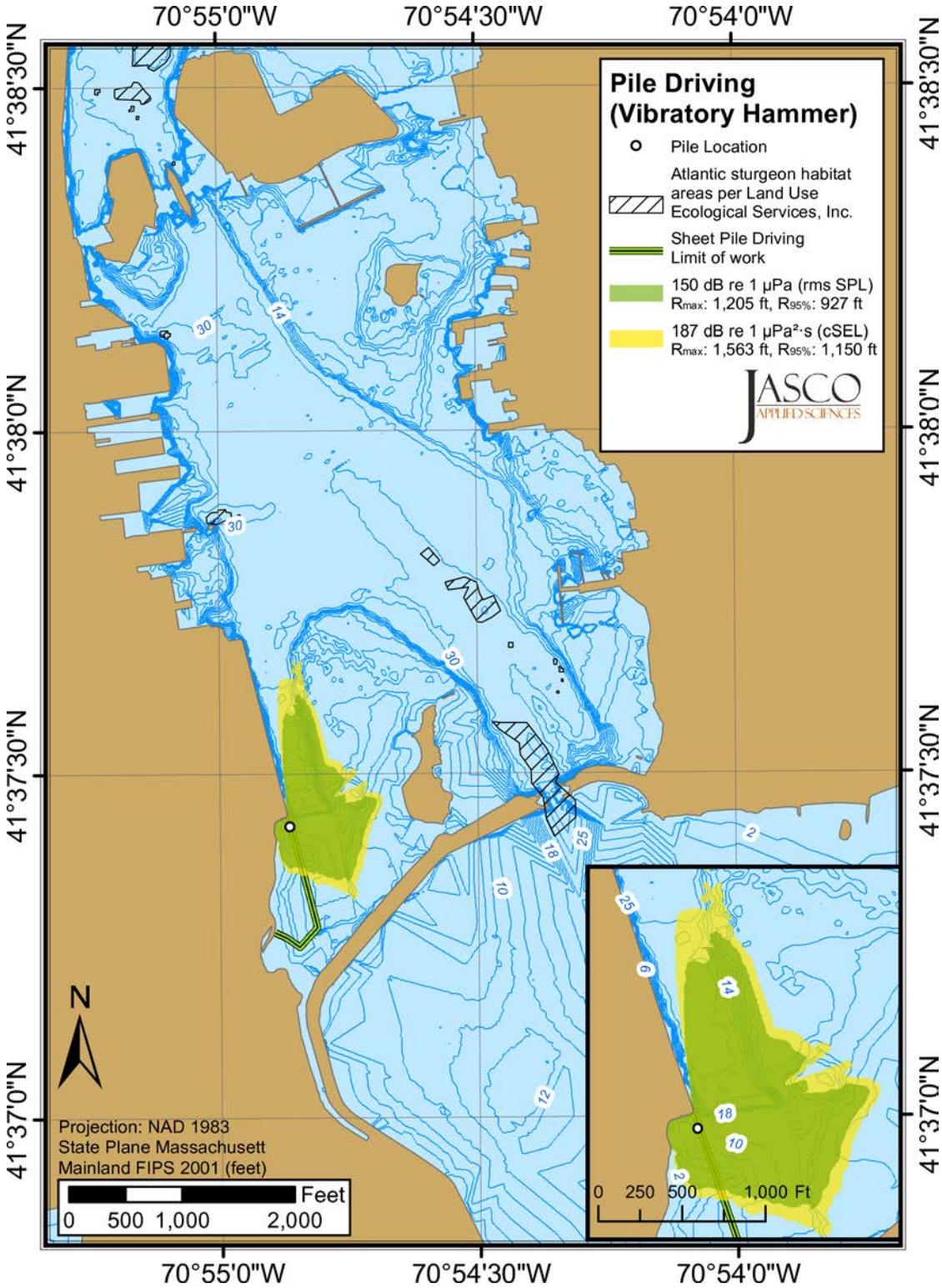

Figure 13. Pile driving with a vibratory hammer at Site 2: Received maximum-over-depth sound level thresholds. Blue contours indicate water depth in feet.

4.2.2. Rock Removal–Non-Explosive

Apex estimates 4 h of non-explosive rock removal operation. Thus, cSELs presented here assume 14 400 s of cutter-head dredge operation in 24 hours. Peak SPL for vibratory pile driving is not expected to reach 206 dB re 1 μPa.

Figures 14 and 16 present contour maps of the modeled rms SPL for non-explosive rock removal (using a cutter-head dredge), while Figures 15 and 17 present contour maps of the modeled sound level thresholds for same type of operation.

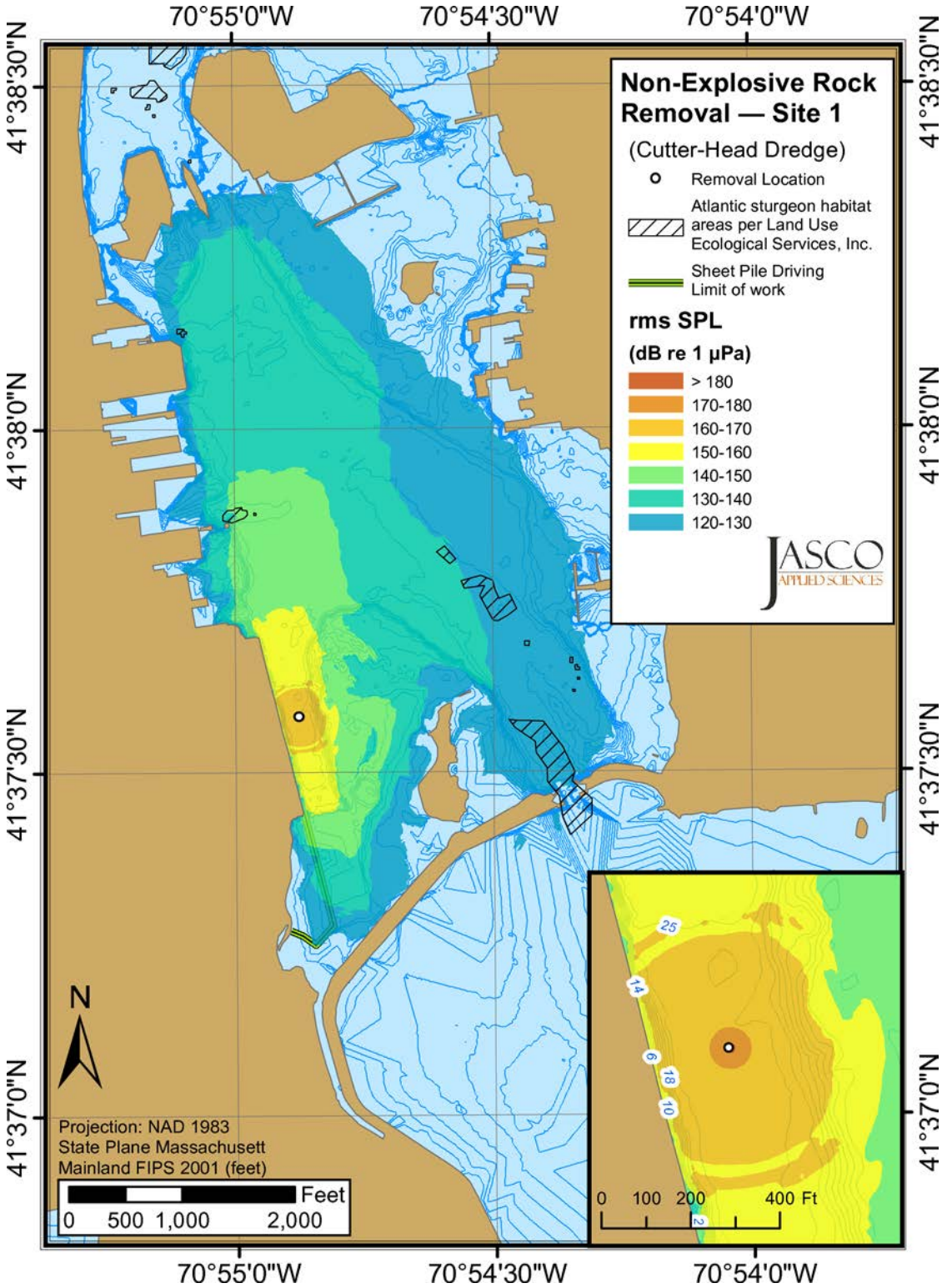

Figure 14. Non-explosive rock removal at Site 1: Received maximum-over-depth root-mean-square (rms) sound pressure levels (SPLs). Blue contours indicate water depth in feet.

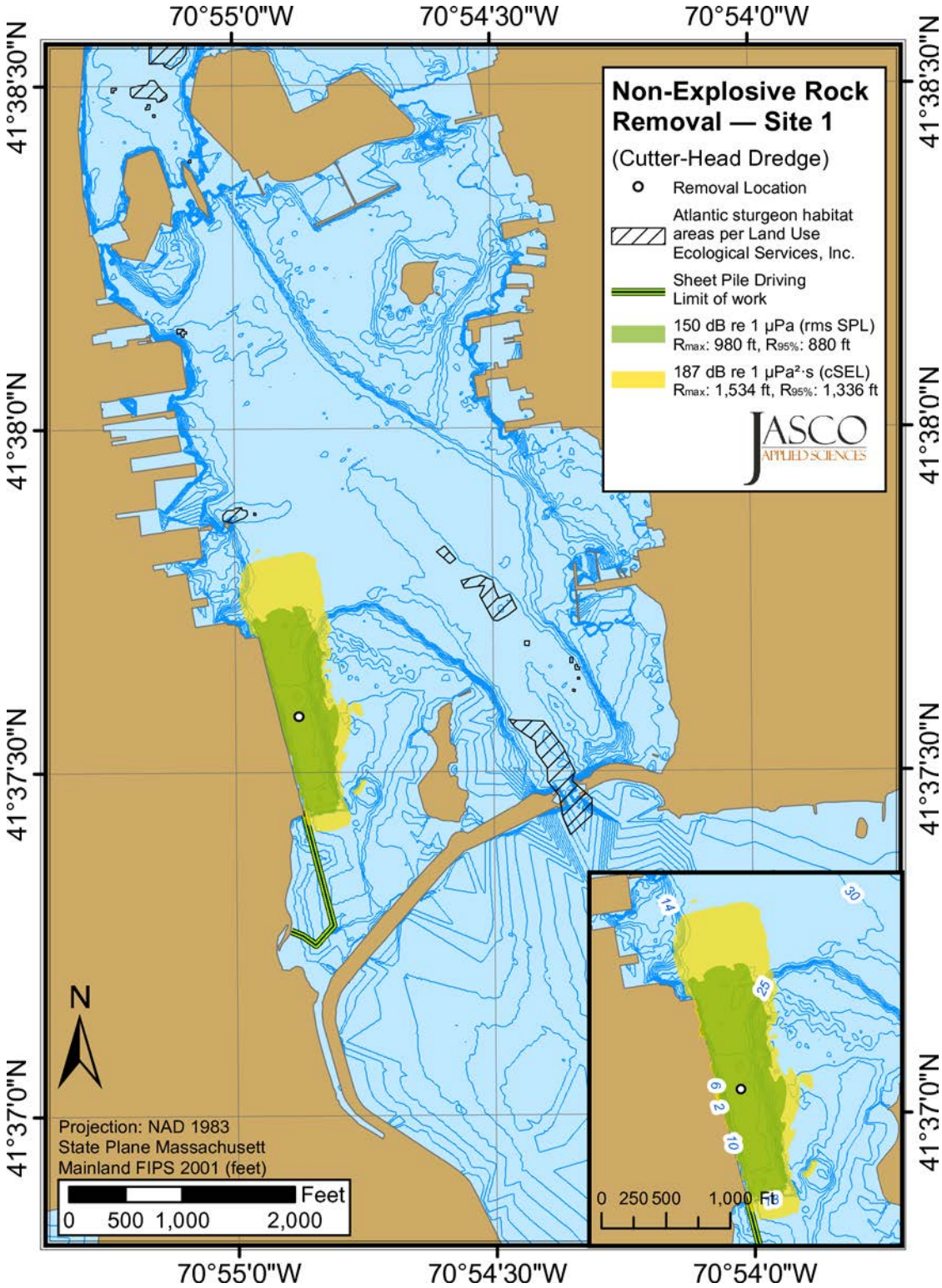

Figure 15. Non-explosive rock removal at Site 1: Received maximum-over-depth sound level thresholds. Blue contours indicate water depth in feet.

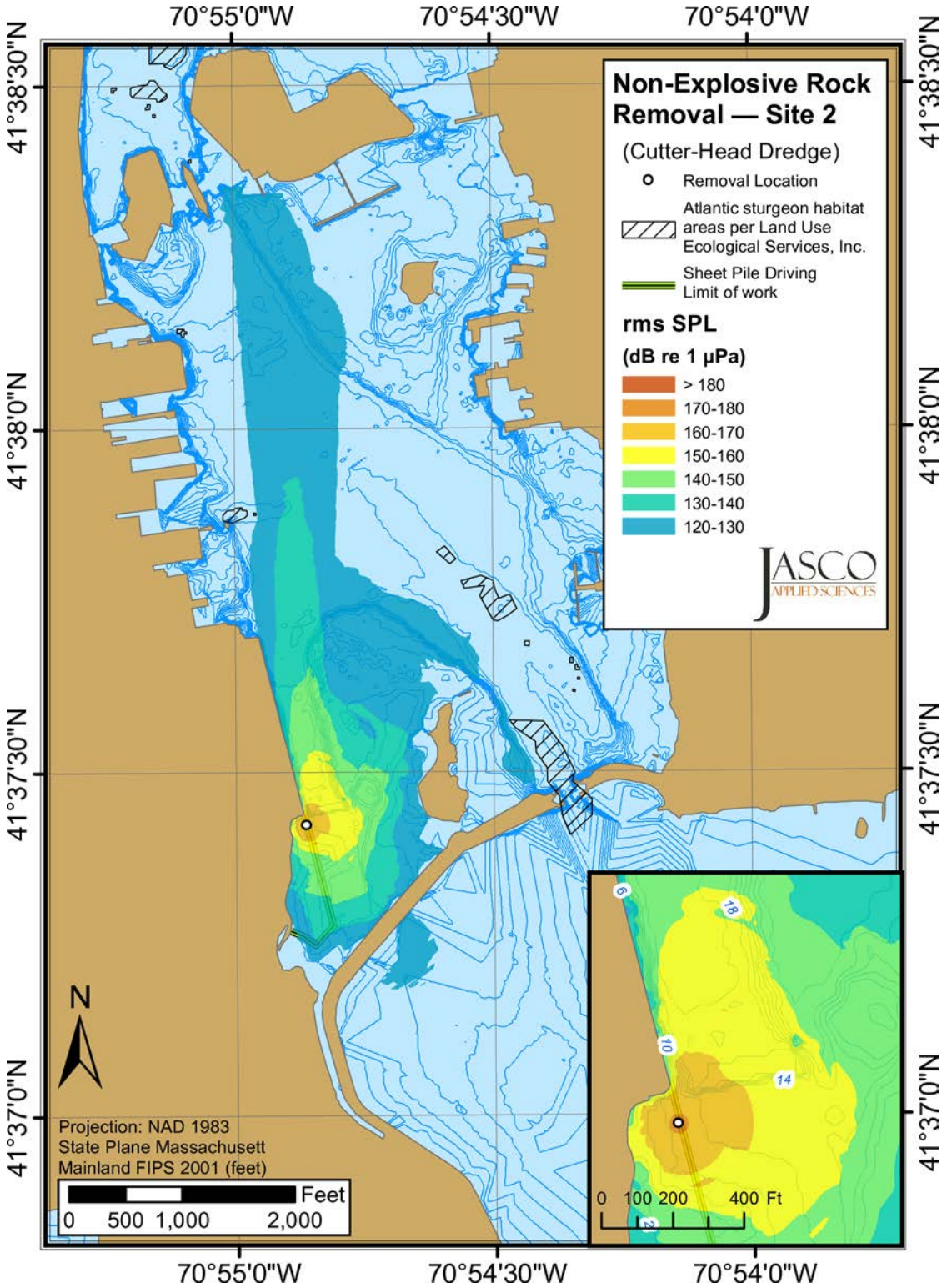

Figure 16. Non-explosive rock removal at Site 2: Received maximum-over-depth root-mean-square (rms) sound pressure levels (SPLs). Blue contours indicate water depth in feet.

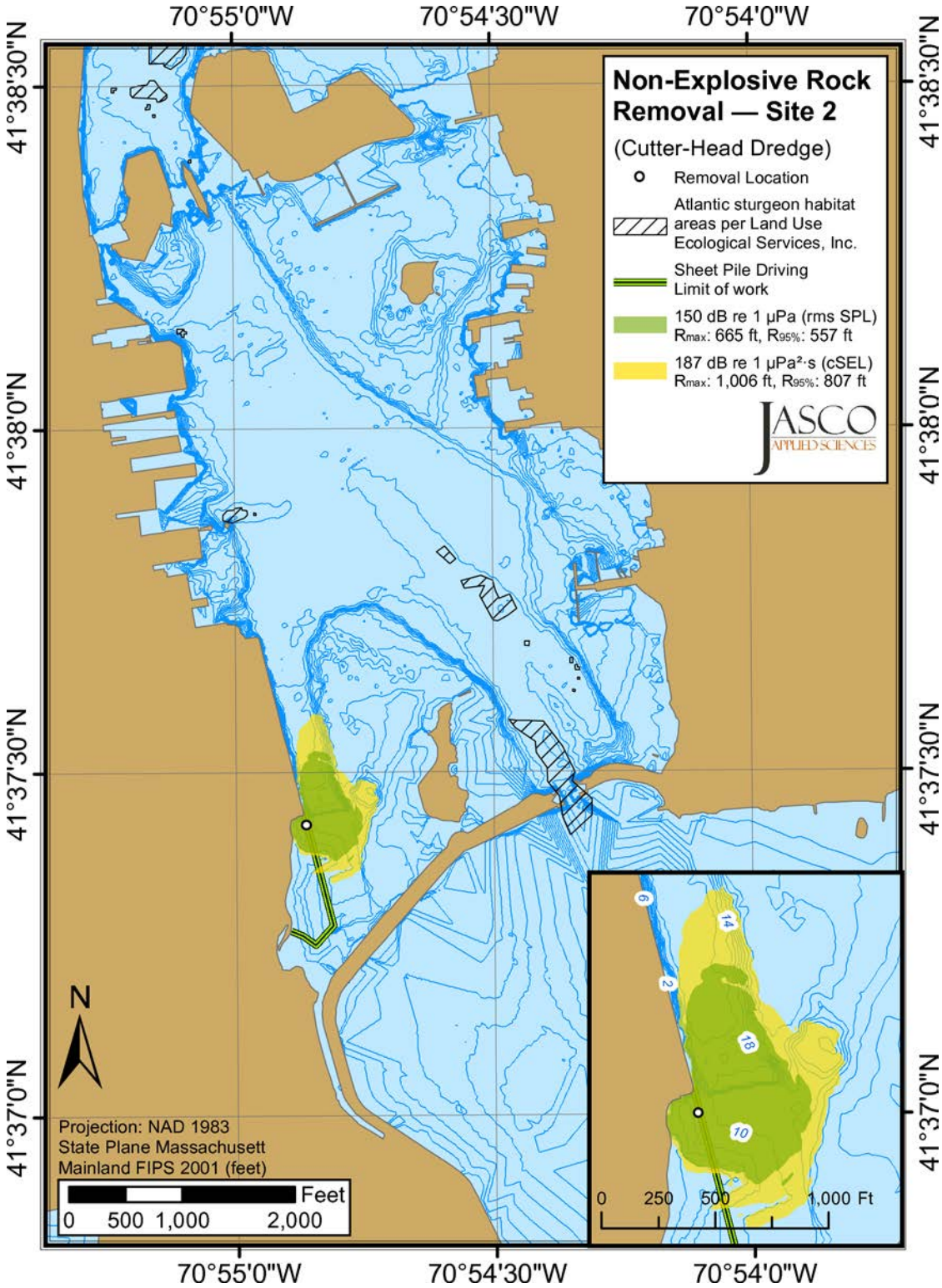

Figure 17. Non-explosive rock removal at Site 2: Received maximum-over-depth sound level thresholds. Blue contours indicate water depth in feet.

4.2.3. Rock Removal–Explosive

The distances to peak pressure and impulse thresholds estimated using the UnderWater Calculator spreadsheet (original and adjusted distances) and ConWep are presented in Tables 6 and 7. The adjusted distances to injury thresholds are also presented as contour maps in Figures 20 and 21. The adjusted effective coefficients used in the UnderWater Calculator spreadsheet range between 2.25% and 5.5%, which are in keeping with expected reductions in effect from the charge being buried in the substrate (USACE 1999). For all charges, the threshold distance for the impulse criterion exceeds that for the peak pressure criterion. These distances to the peak pressure threshold are patently conservative, as they significantly exceed the ConWep model estimates.

As an example, the adjusted distances for the 150 lb charge were calculated as follow:

- ConWep estimates that the zone of injury for a 150 lb charge extends 268 ft from the detonation, based on the impulse level threshold of 18.4 psi·ms (Table 7). For a fixed impulse of 18.4 psi·ms, the efficiency coefficient was reduced until the distance was 291 ft (6% greater than the distance estimated by ConWep), resulting in an efficiency coefficient of 2.25% (Figure 18).
- Using this 2.25% coefficient, the distances was then reduced until the peak pressure level was 75.6 psi; resulting in an adjusted distance to peak pressure of 231 ft (Figure 19; Table 6).

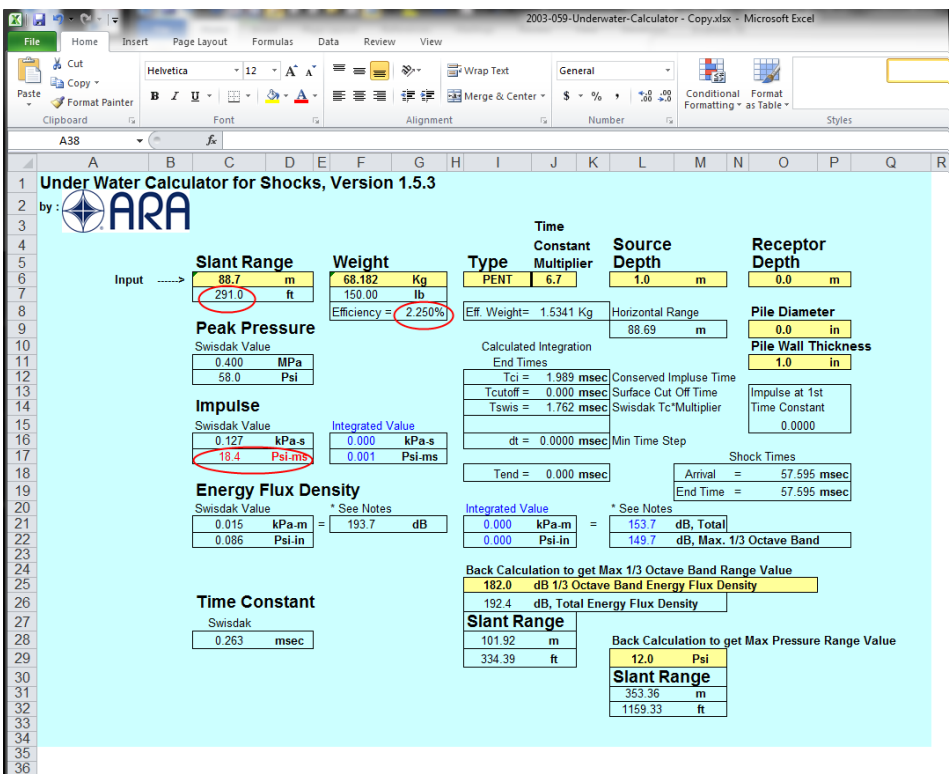

Figure 18. Screenshot of UnderWater Calculator spreadsheet while calculating the adjusted distance (slant range) to the injury criteria of 18.4 psi·ms.

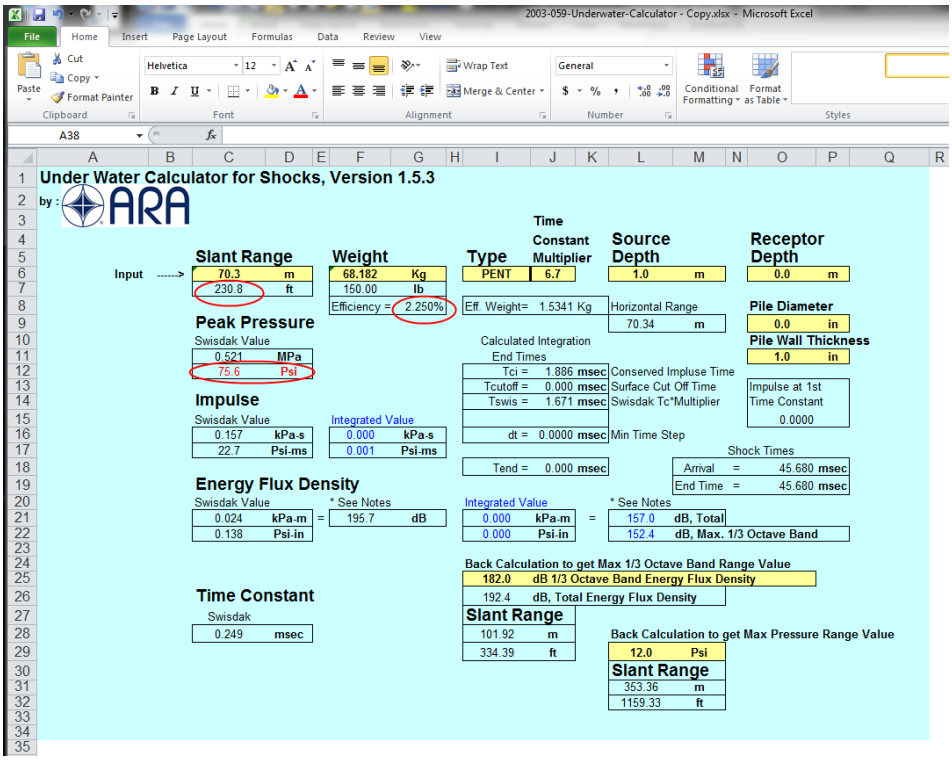

Figure 19. Screenshot of UnderWater Calculator spreadsheet while calculating the adjusted distance (slant range) to the injury criteria of 75.6 psi.

The inputs to ConWep used to calculate the pressure wave characteristics (Section 2.2.3.2) were based on the water depth and geoacoustic properties at Site 2. We estimate nonetheless that the resulting distances to injury thresholds for blasting operations are also applicable to Site 1. The geoacoustic properties of the two areas are very similar and would be modeled with the same parameters. Water depth is the main difference between the sites; the water is 20 ft deep at Site 1 compared to 9 ft at Site 2. With increasing water depth, the time delay between the surface-reflected and direct pressure waves increases, resulting in a longer range to impulse threshold. The precautionary assumptions and conservative margins applied in the numerical estimations, however, accommodate the variability between the two sites.

The modeled distances to impulse levels for injury criteria (18.4 psi·s) can be validly considered as "distances for charge weight per delay" for delays of 25 ms or more. This statement is based on the integration period for the impulse metric as defined as the time elapsed from the onset of the primary pressure wave to its return to ambient, i.e., the duration of the first positive pressure wave. The same integration period is applicable to individual events in a delayed sequence of detonations providing the onset of an event does not overlap the positive phase of the previous one. While the positive pressure phase of an event may last just a few milliseconds, in practice some standard delay guidelines are generally applied to blasting operations to ensure a clear separation under realistic conditions. In the absence of formal directives from NMFS regarding minimum acceptable delays, based on Canadian guidelines for the use of explosives in or near fisheries waters (Wright and Hopky 1998) and results from experiments (Bullard, J. K. 2012), we recommend a minimum time delay of 25 ms between detonations. JASCO's analysis is strictly

limited to the physical estimate of acoustic parameters; it does not attempt to interpret the biological impact of detonations on fish.

Table 6. Distances to peak pressure injury criterion of 75.6 psi.

Charge Weight (lb)	Original distances (ft)	ConWep distances (ft)	Adjusted distances (ft)	Adjusted efficiency coefficient
30	346	46	182	5.5%
50	418	53	201	4.5%
100	552	65	222	3%
130	617	70	228	2.5%
150	659	73	231	2.25%

Table 7. Distances to impulse injury criterion of 18.4 psi•ms.

Charge Weight (lb)	Original distances (ft)	ConWep distances (ft)	Adjusted distances (ft)	Adjusted efficiency coefficient
30	681	166	187	5.5%
50	1017	196	219	4.5%
100	1820	240	268	3%
130	2304	258	283	2.5%
150	2631	268	291	2.25%

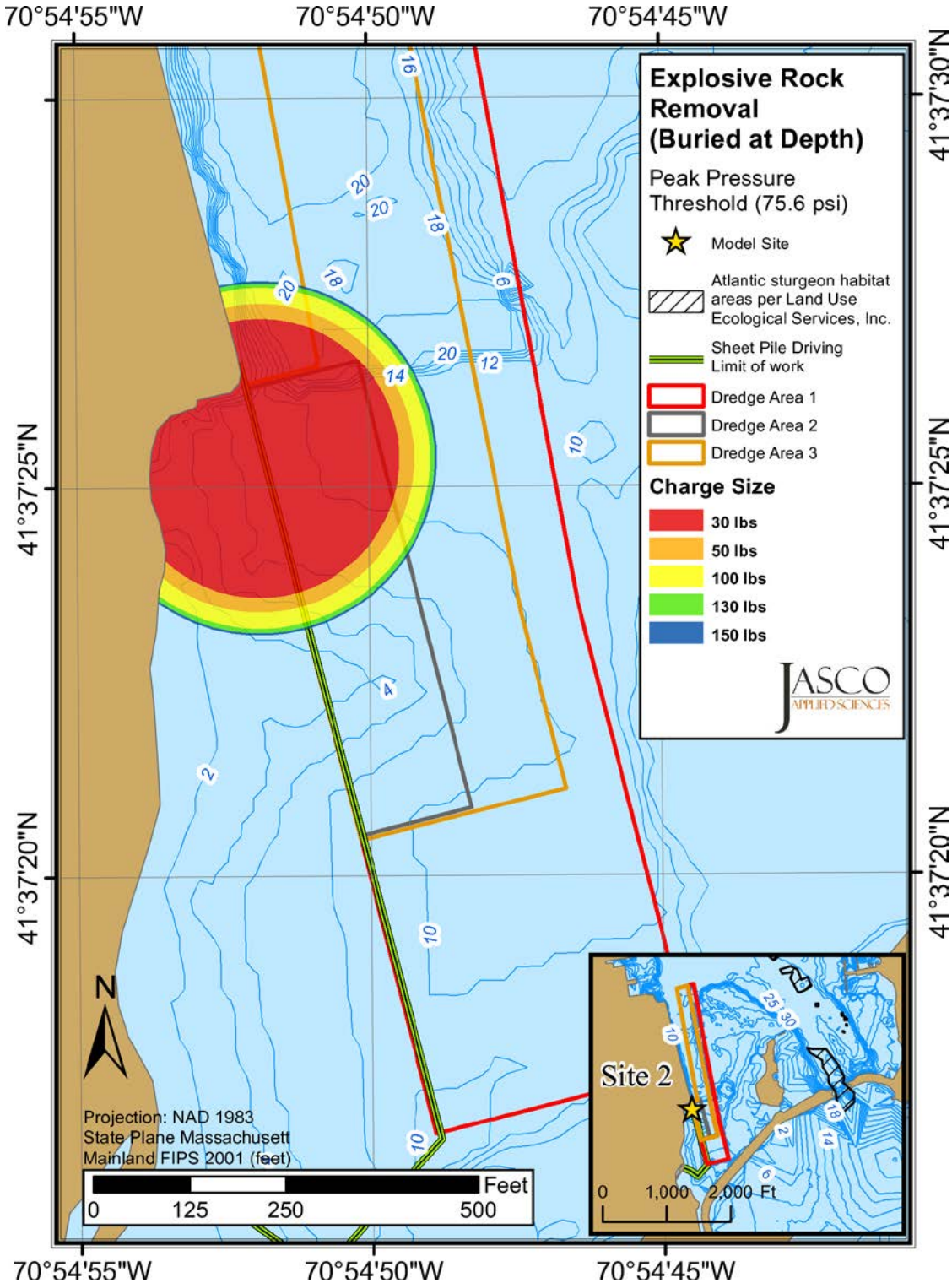

Figure 20. Small scale contour map for explosive charge at Site 2: Peak pressure threshold of 75.6 psi for explosive charges between 30 and 150 lb. Blue contours indicate water depth in feet.

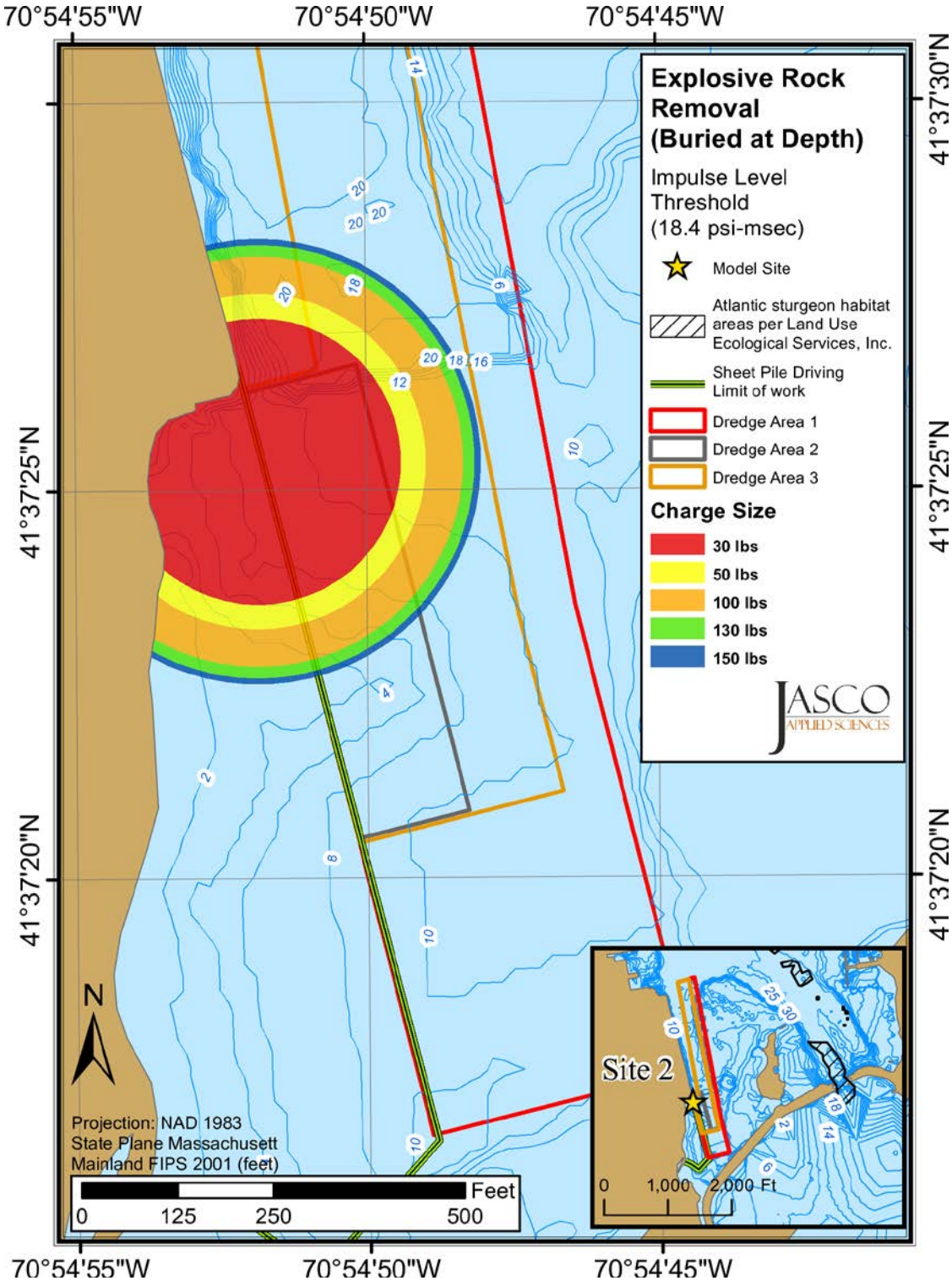

Figure 21. Small scale contour map for explosive charge at Site 2: Impulse level threshold of 18.4 psi·ms for explosive charges between 30 and 150 lb. Blue contours indicate water depth in feet.

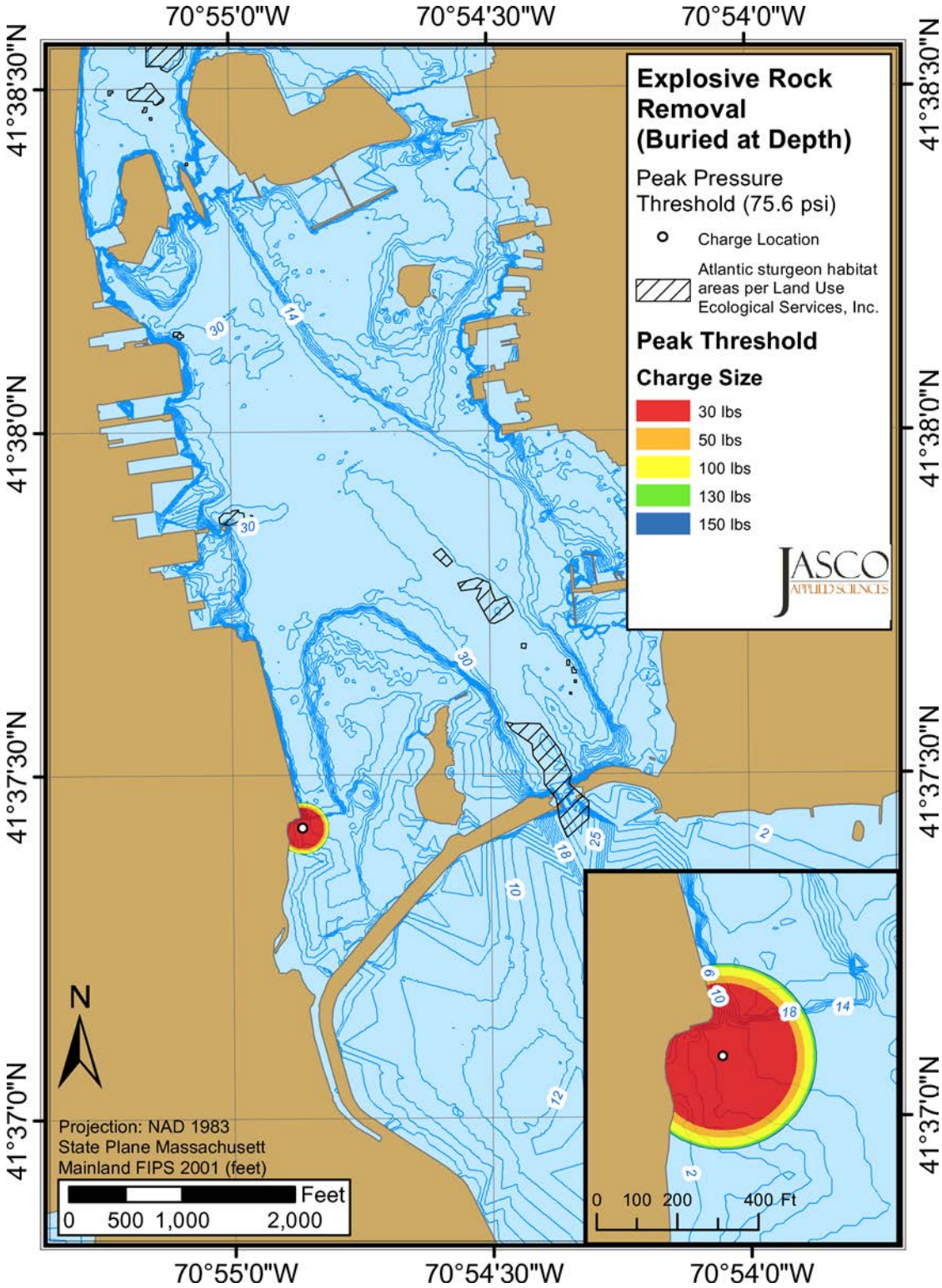

Figure 22. Large scale contour map for explosive charge at Site 2: Peak pressure threshold of 75.6 psi for explosive charges between 30 and 150 lb. Blue contours indicate water depth in feet.

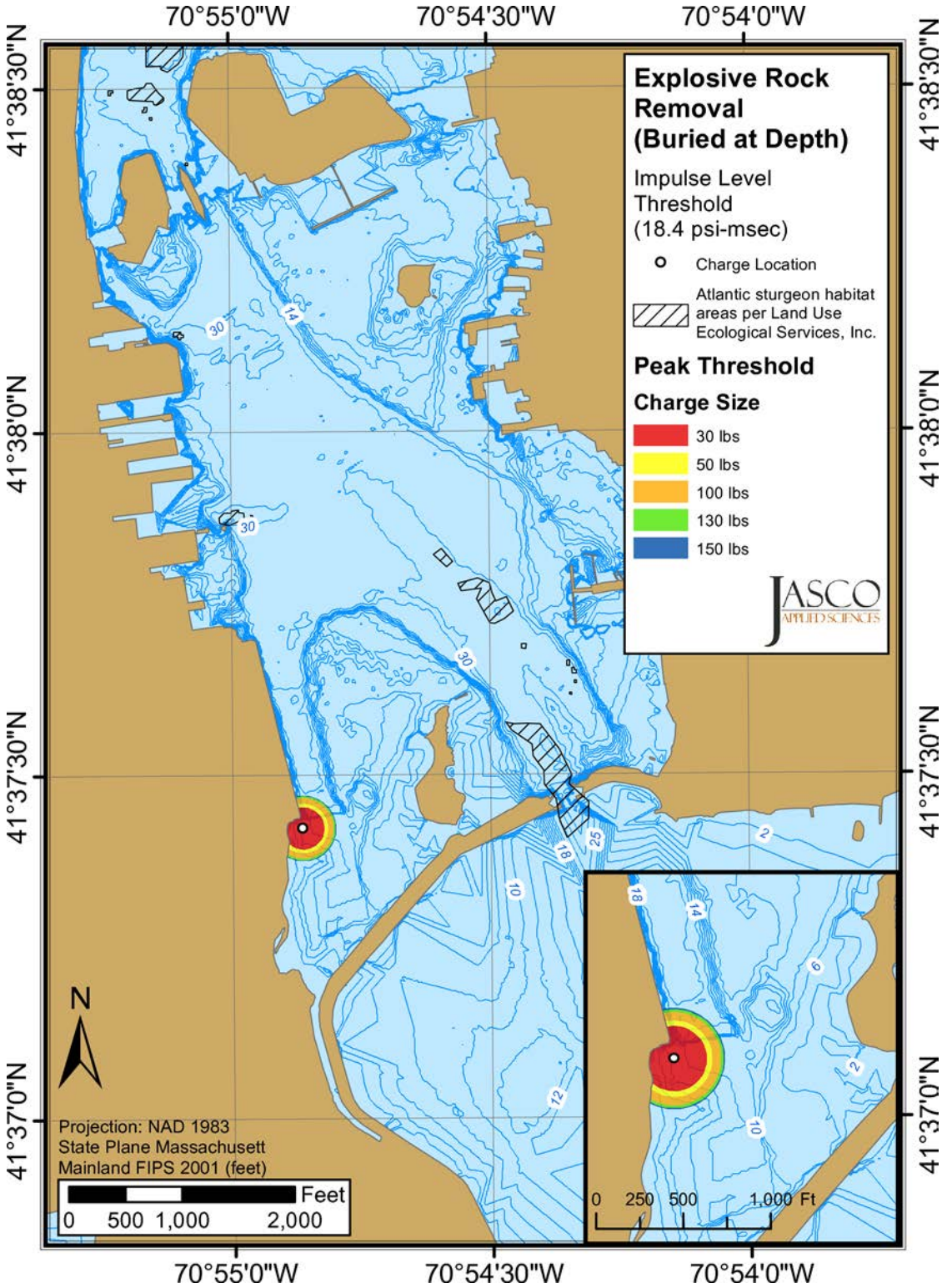

Figure 23. Large scale contour map for explosive charge at Site 2: Impulse level threshold of 18.4 psi·ms for explosive charges between 30 and 150 lb. Blue contours indicate water depth in feet

Literature Cited

Aerts, L., M. Blees, S. Blackwell, C. Greene, K. Kim, D. Hannay, and M. Austin. 2008. Marine mammal monitoring and mitigation during BP Liberty OBC seismic survey in Foggy Island Bay, Beaufort Sea, July-August 2008: 90-day report. LGL Rep. P1011-1. Prepared by LGL Alaska Research Associates Inc., LGL Ltd., Greeneridge Sciences Inc. and JASCO Applied Sciences Ltd. for BP Exploration Alaska.

Austin, M., J. Delarue, H.A. Johnston, M. Laurinolli, D. Leary, A. MacGillivray, C. O'Neill, H. Sneddon, and G. Warner. 2009. *NaiKun Offshore Wind Energy Project Environmental Assessment*, Volume 4–Noise and Vibration. Technical report for NaiKun Wind Development Inc. by JASCO Applied Sciences.

Barton, N. 2007. *Rock Quality, Seismic Velocity, Attenuation, and Anisotropy*. Taylor & Francis, CIP Bath Press. 729 p.

Blackwell, S.B., R.G. Norman, C.R. Greene Jr., and W.J. Richardson. 2007. Acoustic measurements. (Chapter 4) In: Marine Mammal Monitoring and Mitigation during Open Water Seismic Exploration by Shell Offshore Inc. in the Chukchi and Beaufort Seas, July–September 2006: 90-Day Report. LGL Report P891-1. Report by LGL Alaska Research Associates Inc. and Greeneridge Sciences Inc. for Shell Offshore Inc., National Marine Fisheries Service (US), and US Fish and Wildlife Service. pp 4-1 to 4-52.

Betke, K. 2008. Minderung von Unterwassergeräuschen beim Bau von OffshoreWEA, BSH-Workshop FINO3, Hamburg, 8 Oct. 2008.

Bullard, J.K. 2012. RE: Route 52 Causeway Replacement & Somers Point Circle Elimination Contract B. Personal communication with National Marine Fisheries Service (NMFS).

CALTRANS. 2009. *Technical guidance for assessment and mitigation of the hydroacoustic effects of pile driving on Fish.* Technical report prepared by ICF Jones & Stokes and Illingworth and Rodkin, Inc, for California Department of Transportation, Sacramento CA.

Carnes, M.R. 2009. Description and Evaluation of GDEM-V 3.0. NRL Memorandum Report 7330-09-9165. US Naval Research Laboratory, Stennis Space Center, MS. 21 p.

[CEDA] Central Dredging Association. 2011. *Underwater Sound in Relation to Dredging*. CEDA Position Paper–7. 6 p. http://www.dredging.org/documents/ceda/html_page/2011-11_ceda_positionpaper_underwatersound_v2.pdf

Collins, M.D. 1993. A split-step Pade solution for the parabolic equation method. *Journal of the Acoustical Society of America* 93(4):1736-1742.

Collins, M.D., R.J. Cederberg, D.B. King, and S.A. Chin-bing. 1996. Comparison of algorithms for solving parabolic wave equations. *Journal of the Acoustical Society of America* 100:178–182.

Coppens, A.B. 1981. Simple equations for the speed of sound in Neptunian waters. *Journal of the Acoustical Society of America* 69:862-863.

[CSA] Continental Shelf Associates Inc. 2004. *Explosive removal of offshore structures -information synthesis report*. OCS Study MMS 2003-070. U.S. Department of the Interior, Minerals Management Service, Gulf of Mexico OCS Region, New Orleans, LA. 181 p.

Dickerson, C., K.J. Reine, and D.G. Clarke. 2001. *Characterization of underwater sounds produced by bucket dredging operations*. DOER Technical Notes Collection (ERDC TN-DOER-E14), U.S. Army Engineer Research and Development Center, Vicksburg, MS. http://www.fakr.noaa.gov/protectedresources/whales/beluga/development/portofanc/erdc_dredge_noise_2001.pdf

Dzwilewski, P.T. and G. Fenton. 2003. Shock wave/sound propagation modeling results for calculating marine protected species impact zones during explosive removal of offshore structures. U.S. Dept. of the Interior, Minerals Management Service, Gulf of Mexico OCS Region, New Orleans, LA. OCS Study MMS 2003-059. 34 p. http://www.boem.gov/BOEM-Newsroom/Library/Publications/2003/2003-059.aspx

Ellis, D. and S. Hughes. 1989. *Estimates of sediment properties for ARPS*. DREA Memorandum TIAT-27. Defence Research Establishment Atlantic, Dartmouth, NS. 2 p.

Erbe, C. 2009. Underwater noise from pile driving in Moreton Bay, Qld. *Acoustics Australia* 37(3):87-92.

[FHWG] Fisheries Hydroacoustic Working Group. 2008. *Agreement in Principle for Interim Criteria for Injury to Fish from Pile Driving Activities. Memorandum*. http://www.wsdot.wa.gov/NR/rdonlyres/4019ED62-B403-489C-AF05-5F4713-D663C9/0/BA_InterimCriteriaAgree.pdf

Fisher, F.H. and V.P. Simmons. 1977. Sound absorption in sea water. *Journal of the Acoustical Society of America* 62(3):558-564.

Funk, D., D. Hannay, D. Ireland, R. Rodrigues, and W. Koski (eds.). 2008. Marine Mammal Monitoring and Mitigation during Open Water Seismic Exploration by Shell Offshore Inc. in the Chukchi and Beaufort Seas, July–November 2007: 90-Day Report. LGL Report P969-1. Prepared by LGL Alaska Research Associates Inc., LGL Ltd., and JASCO Research Ltd. for Shell Offshore Inc., National Marine Fisheries Service (US), and US Fish and Wildlife Service. 218 p. http://www-static.shell.com/static/usa/downloads/alaska/shell2007_90-d_final.pdf.

Gaboury, I., M. Zykov, S. Carr, and D. Hannay. 2007a. *Ladd deepwater marine coal terminal: assessment of underwater noise.* Technical report for DRven Corporation by JASCO Applied Sciences, 65 p.

Gaboury, I., R. Gaboury, and S. Carr. 2007b. *Downeast LNG import terminal: assessment of underwater noise impacts*. Technical report for Resource Systems Engineering Inc. by JASCO Research Ltd, 45 p.

Hamilton, E.L. 1980. Geoacoustic modeling of the sea floor. *Journal of the Acoustical Society of America* 68:1313-1340.

Hannay, D.E. and R.G. Racca. 2005. *Acoustic Model Validation*. Document 0000-S-90-04-T-7006-00-E, Revision 02. Technical report for Sakhalin Energy Investment Company Ltd. by JASCO Research Ltd. 34 p. http://www.sakhalinenergy.com/en/documents/doc_33_jasco.pdf

Hannay, D., A.O. MacGillivray, M. Laurinolli, and R. Racca. 2004. *Sakhalin Energy–Source Level Measurements from 2004 Acoustics Programme*. Report by JASCO Research Ltd., Victoria, BC.

Hyde, D. W. 1988. User's guide for microcomputer programs ConWep and FunPro applications of TM 5-855-1. "Fundamentals of protective design for conventional weapons".

Hyde, D. W. 1992. Conventional weapons effect computer program, US Waterways Experiment Station Instructional Report SL-88-1. U.S. Army Corps of Engineers.

Illingworth and Rodkin, Inc. 2007. *Compendium of Pile Driving Sound Data* (Appendix I). Prepared for The California Department of Transportation. 129 p. http://www.dot.ca.gov/hq/env/bio/files/pile_driving_snd_comp9_27_07.pdf

Ireland, D.S., R. Rodrigues, D. Funk, W. Koski, and D. Hannay. 2009. Marine mammal monitoring and mitigation during open water seismic exploration by Shell Offshore Inc. in the Chukchi and Beaufort Seas, July–October 2008: 90-day report. LGL Rep. P1049-1. Prepared by LGL Alaska Research Associates Inc., LGL Ltd., and JASCO Applied Sciences Ltd. for Shell Offshore Inc, Nat. Mar. Fish. Serv., and U.S. Fish and Wild. Serv. 277 p. plus appendices.

MacGillivray, A., G.R. Warner, R. Racca, and C. O'Neill. 2011. *Tappan Zee Bridge Construction Hydroacoustic Noise Modeling: Final Report.* Report by JASCO Applied Sciences for AECOM. 63 p. http://www.newnybridge.com/documents/feis/vol2/f-4a-tzb-construction-hydroacoustic-noise-modeling.pdf

Malme, C.I., P.R. Miles, G.W. Miller, W.J. Richardson, D.G. Roseneau, D.H. Thomson, and C.R. Greene Jr. 1989. Analysis and ranking of the acoustic disturbance potential of petroleum industry activities and other sources of noise in the environment of marine mammals in Alaska. BBN Systems and Technologies Corporation for Minerals Management Service U.S. Department of the Interior.

McGlaun, J.M., S.L. Thompson, and M.G. Elrick. 1990. CTH: A three-dimensional shock wave physics code. *International Journal of Impact Engineering* 10:351-360.

McHugh, O., M. Fraker, B. Wheeler, M. Austin, M. Zykov, and M. Laurinolli. 2007. *Potential Acoustic Impacts to Killer Whales Associated With Construction Dredging at DP3.* PROJECT NO. 1021281. Report prepared for Vancouver Port Authority by Jacques Whitford-AXYS and JASCO Research Ltd. 53 p.

Miles, P.R., C.I. Malme, and W.J. Richardson. 1987. Prediction of Drilling Site-Specific Interaction of Industrial Acoustic Stimuli and Endangered Whales in the Alaskan Beaufort Sea. OCS Study. MMS 87-0084. BBN Report No. 6509. Anchorage. AK: USDOI. MMS, Alaska OCS Region. 341 p.

Mosher, M. 1999. *Cape Fear River blasting mitigation test: Results of caged fish necropsies.* Final Report to CZR, Inc. under contract to U.S. Army Corps of Engineers, Wilmington District.

Mouy, X., and M. Zykov. 2009. *Underwater acoustic monitoring of pile driving activities in the Penobscot River, Bangor, Main*. Version 1.2, Technical report for RMT Inc. by JASCO Applied Sciences.

Nehls, G., K. Betke, S. Eckelmann, and M. Ros. 2007. Assessment and costs of potential engineering solutions for the mitigation of the impacts of underwater noise arising from the construction of offshore windfarms. Technical report for COWRIE by BioConsult SH.

Nützel, B. 2008. Untersuchungen zum Schutz von Schweinswalen vor Schockwellen (Investigations to protect harbour porpoises from shock waves). Technischer Bericht TB 2008–7, FWG. Kiel, Germany.

O'Neill, C., D. Leary, and A. McCrodan. 2010. Sound Source Verification. (Chapter 3) *In*: Blees, M.K., K.G. Hartin, D.S. Ireland, and D. Hannay (eds.). *Marine mammal monitoring and mitigation during open water seismic exploration by Statoil USA E&P Inc. in the Chukchi Sea, August-October 2010: 90-day report*. LGL Report P1119. Prepared by LGL Alaska Research Associates Inc., LGL Ltd., and JASCO Applied Sciences Ltd. for Statoil USA E&P Inc., National Marine Fisheries Service (US), and US Fish and Wildlife Service. pp. 3-1 to 3-34.

Porter, M.B. and Y.-C. Liu. 1994. Finite-element ray tracing. *In*: Lee, D. and M.H. Schultz (eds.). *Proceedings of the International Conference on Theoretical and Computational Acoustics*. Volume 2. World Scientific Publishing Co. pp 947-956.

Robinson, S.P., P.D. Theobald, G. Hayman, L.S. Wang, P.A. Lepper, V. Humphrey, and S. Mumford. 2011. *Measurement of noise arising from marine aggregate dredging operations.* MALSF. MEPF Ref no. 09/P108.

Rodriguez, E., C.S. Morris, Y.J.E. Belz, E.C. Chapin, J.M. Martin, W. Daffer, and S. Hensley. 2005. *An assessment of the SRTM topographic products.* JPL D-31639. Jet Propulsion Laboratory Pasadena, CA.

Southall, B.L., A.E. Bowles, W.T. Ellison, J.J. Finneran, R.L. Gentry, C.R. Greene Jr., D. Kastak, and D.R. Ketten. 2007. Marine mammal noise exposure criteria: Initial scientific recommendations. *Aquatic Mammals* 33(4):411–521.

Swisdak, Jr., M.M. 1978. *Explosion effects and properties: Part II - Explosion effects in water.* Naval Surface Weapons Center, Silver Spring, MD. NSWC/WOL TR 76-116. http://www.dtic.mil/cgi-bin/GetTRDoc?Location=U2&doc=GetTRDoc.pdf&AD=ADA056694

Teague, W.J., M.J. Carron, and P.J. Hogan. 1990. A comparison between the Generalized Digital Environmental Model and Levitus climatologies. *J. Geophys. Res.* 95(C5):7167-7183.

[USACE] U.S. Army Corps of Engineers, Waterways Experiment Station. 1999. Draft, Analysis of Water Shock Data and Bubble Screen Effectiveness on the Blast Effect Mitigation Test Series, Wilmington Harbor, NC. Vicksburg, MS. Prepared by Denis Rickman for U.S. Army Corps of Engineers, Wilmington District, Wilmington, NC.

Vagle, S. 2003. *On the impact of underwater pile-driving noise on marine life.* Technical report by Institute of Ocean Sciences, DFO/Pacific, Ocean Science and Productivity Division.

Warner, G., C. Erbe, and D. Hannay. 2010. Underwater sound measurements. (Chapter 3) *In*: Reiser, C.M., D.W. Funk, R. Rodrigues, and D. Hannay (eds.). *Marine Mammal Monitoring and Mitigation during Open Water Shallow Hazards and Site Clearance Surveys by Shell Offshore Inc. in the Alaskan Chukchi Sea, July-October 2009: 90-Day Report.* LGL Report P1112-1. Report by LGL Alaska Research Associates Inc. and JASCO Applied Sciences for Shell Offshore Inc., National Marine Fisheries Service (US), and US Fish and Wildlife Service. pp 3-1 to 3-54. http://www-static.shell.com/static/usa/downloads/alaska/report_2009_shell_90-d_report_plus_appendices.pdf.

Wright, D.G., and G.E. Hopky. 1998. Guidelines for the use of explosives in or near Canadian fisheries waters. Can. Tech. Rep. Fish. Aquat. Sci. 2107: iv + 34p. http://www.dfo-mpo.gc.ca/Library/232046.pdf

WSDOT. 2010a. Underwater sound levels associated with driving steel piles for the State Route 520 bridge replacement and HOV project pile installation test program. Technical report for Washington State Department of Transportation by Illingworth and Rodkin Inc.

WSDOT. 2010b. *Biological Assessment Preparation Advanced Training Manual*. Technical report by Washington State Department of Transportation.